

Review

Nanomaterials-Based Electrochemical Sensors for In Vitro and In Vivo Analyses of Neurotransmitters

Sharmila Durairaj, Boopathi Sidhureddy, Joseph Cirone and Aicheng Chen *

Electrochemical Technology Centre, Department of Chemistry, University of Guelph, 50 Stone Road East, Guelph, ON N1G 2W1, Canada; sduraira@uoguelph.ca (S.D.); bsidhure@uoguelph.ca (B.S.); jcirone@uoguelph.ca (J.C.)

* Correspondence: aicheng@uoguelph.ca; Tel.: +1-519-824-4120 (ext. 54764)

Received: 30 July 2018; Accepted: 27 August 2018; Published: 1 September 2018



Abstract: Neurotransmitters are molecules that transfer chemical signals between neurons to convey messages for any action conducted by the nervous system. All neurotransmitters are medically important; the detection and analysis of these molecules play vital roles in the diagnosis and treatment of diseases. Among analytical strategies, electrochemical techniques have been identified as simple, inexpensive, and less time-consuming processes. Electrochemical analysis is based on the redox behaviors of neurotransmitters, as well as their metabolites. A variety of electrochemical techniques are available for the detection of biomolecules. However, the development of a sensing platform with high sensitivity and selectivity is challenging, and it has been found to be a bottleneck step in the analysis of neurotransmitters. Nanomaterials-based sensor platforms are fascinating for researchers because of their ability to perform the electrochemical analysis of neurotransmitters due to their improved detection efficacy, and they have been widely reported on for their sensitive detection of epinephrine, dopamine, serotonin, glutamate, acetylcholine, nitric oxide, and purines. The advancement of electroanalytical technologies and the innovation of functional nanomaterials have been assisting greatly in in vivo and in vitro analyses of neurotransmitters, especially for point-of-care clinical applications. In this review, firstly, we focus on the most commonly employed electrochemical analysis techniques, in conjunction with their working principles and abilities for the detection of neurotransmitters. Subsequently, we concentrate on the fabrication and development of nanomaterials-based electrochemical sensors and their advantages over other detection techniques. Finally, we address the challenges and the future outlook in the development of electrochemical sensors for the efficient detection of neurotransmitters.

Keywords: electrochemical analysis; neurotransmitters; in vitro and in vivo detection; nanomaterials

1. Introduction

In multicellular organisms, the nervous system transmits information generated in the brain to the entire body [1]. In this process, nerve cells transfer signals from neurons to targeted neuronal chemical synapses. This signal transfer occurs electrically and chemically between nerve cells. In brief, firstly, electrical signals are transmitted along the cell membrane within cells. Secondly, the electrical signals are converted into chemical signals for communication between cells. These chemical signals are conveyed by small messenger molecules, called neurotransmitters, which drive the behavioral, cognitive, and emotional states of an organism. They also have impact on muscle movement and heart rate, while regulating sleep, memory, and learning. There are different types of neurotransmitters that are described as amino acids, peptides, monoamines, gas transmitters, trace amines, and purines. In current analytical research, neurochemical quantification has led to many enhancements toward the understanding of the biochemistry of the nervous system. Abnormal neurotransmitter levels, such as

degenerative diseases, mental disorders, depression, and many other health issues, may significantly affect physiological and behavioral processes. The quantitative detection of neurotransmitters has the strong potential to aid in the development of medical diagnostics and therapeutics [2].

Spectroscopic, chromatographic, and electrochemical strategies are the most commonly used analytical methods for the detection of neurotransmitters. For instance, optical spectroscopy, liquid chromatography, capillary electrophoresis separations, mass spectrometry, microelectrodes, electrochemical sensors, and biosensors are widely employed techniques for the detection of neurochemicals [3]. To utilize spectroscopic and chromatographic techniques, sample separation and purification, which are tedious and time consuming, are required prior to measurements. Moreover, in the optical-based techniques, sample preparation is an additional step and is involved with other chemical species, such as fluorescent dyes or metal complexes, for the selective and sensitive detection of neurotransmitters [4]. The applicability of these technologies are further limited in *in vivo* measurements due to complex instrumentation, difficulties in miniaturization, and high cost. In contrast, electrochemical-based approaches with microelectrodes might be employed either directly or following sample purification via ultra-dialysis, centrifugation, or perfusion methods [5]. The electrochemical analysis of neurotransmitters involves the measurement of changes in currents when an electrode potential is applied. In principle, if a neurotransmitter can be oxidized electrochemically, it should be detected and monitored through *in vivo* or *in vitro* electrochemical measurements. *In vitro* studies, conducted outside of a living organism in a controlled environment, are commonly used for electrochemical measurements. These studies prove the ability of a certain nanomaterial to detect a given neurotransmitter but are not reflective of the complexity of a true living organism. For this reason, *in vitro* studies may not be a truly accurate description of the nanomaterials' performance within a living organism. *In vivo* studies are conducted within living tissue and are typically more complicated than *in vitro* measurements. *In vivo* measurements are more reflective of the true performance of the nanomaterial being studied. Short-term analysis may confirm the feasibility of a proposed nanomaterials-based electrochemical sensor, but long-term measurements should be performed to ensure the stability and toxicity of a nanomaterial in a living organism. The integration of both *in vivo* and *in vitro* measurements would provide important information regarding the ability of a nanomaterial to detect neurotransmitters. To detect and monitor neurotransmitters, various electroanalytical methods have been employed such as cyclic voltammetry (CV), differential pulse voltammetry (DPV), squarewave voltammetry (SWV), amperometry, and so forth [6,7].

CV is the most extensively used technique for initial electrochemical studies, in which potential is applied to the electrode in a triangular waveform and the resulting current is measured. Based on cyclic voltammograms, qualitative and quantitative information of analytes can be provided by means of measuring the redox peak potential and peak current. CV is also employed to obtain thermodynamic and mechanistic information related to electrochemical reactions. Akin to CV, linear sweep voltammetry (LSV) is also a very useful tool to elucidate reaction mechanisms and electrode processes. These techniques are practically useful for studying more complex reactions of various biologically important molecules, including, but not limited to, neurotransmitters. However, in these techniques, the inherent non-faradaic process contribution is unavoidable, and it may significantly limit the detection of analytes. Thus, in order to measure the small faradaic current, the non-faradic current should be subtracted. Moreover, to minimize the non-faradic contribution toward lowering the limit of detection, differential pulse voltammetry (DPV) and squarewave voltammetry (SWV) have been employed in electrochemical sensing and biosensing of disease-related biomarkers and chemical contaminants [8]. Scanning electrochemical microscopy (SECM) is also another important technique that has been used to detect and monitor neurotransmitters. For instance, dopamine released from single cells was successfully monitored using SECM [9].

Amperometry is another useful electrochemical technique for the detection of neurotransmitters. In amperometry, the electrode is held at a constant potential to enable the oxidation or reduction of an analyte of interest where a mass transport limited current is generated. The mass transport limited

currents may be converted into concentrations using calibration factors obtained from standards of known concentrations. This technique might detect neurotransmitters at the sub-nanomolar concentration range. As some biomolecules (e.g., proteins) may not be electrochemically oxidized/reduced directly, mediators may be utilized for the electrochemical detection of the targeted molecules. However, these techniques may be subject to some complications, such as mutual interference due to the oxidation of multiple biomolecules at the same potential, inherent low concentration, and possible fouling. To overcome these challenges, considerable efforts have been invested to develop nanomaterials-based electrochemical sensors for the sensitive detection of biologically significant molecules for medical applications [4,8]. In this review article, we mainly focus on the development of various functional nanomaterials-based electrochemical sensors for the detection of neurotransmitters.

A variety of nanomaterials have been explored for the electrochemical detection of neurochemicals, as illustrated in Figure 1. For instance, noble metals (e.g., Au, Ag, Pt, and Pd), non-noble metal oxides (e.g., Fe_2O_3 , FeMoO_4 , NiO, and Co_3O_4), polymers (e.g., polypyrrole, Nafion, and poly(3,4-ethylenedioxythiophene) (PEDOT)), carbon-based nanomaterials (carbon nanotubes (CNT), graphene, and carbon fiber), and the combination of these materials have been used for in vitro and/or in vivo detection of neurotransmitters [9–12]. The size, shape, and synthetic procedure of the functional nanomaterials may considerably influence the sensing performance. The advancement of synthetic chemistry and the evolution of nanoscience and technology have greatly assisted in the fabrication of sensitive and selective sensing platforms. Numerous methods have been reported for the synthesis of noble metal-based nanoparticles, such as chemical reduction, hydrothermal, solvothermal, and thermal annealing methods, with controlled size and shape [13–17]. Among the noble metal-based nanomaterials, gold nanoparticles have been widely exploited for biomedical applications due to their peculiar properties such as chemical, optical, electrical, and catalytic biocompatibility and its ability to conjugate with biomolecules [18]. Silver nanoparticles have also been extensively explored for practical applications due to their highly selective and sensitive performance towards the detection of biomolecules [19–21]. In addition, various non-noble metal-based metal/metal oxides have been fabricated and tested for the in vitro analysis of neurotransmitters.

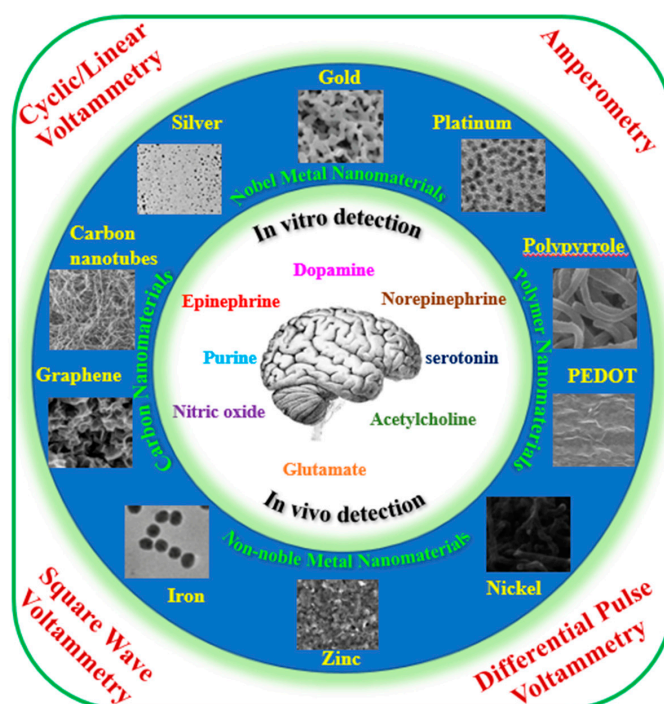


Figure 1. Schematic representation of the application of various nanoparticles for the in vitro and in vivo detection of neurotransmitters using different electrochemical methods.

Furthermore, carbon-based nanomaterials have been extensively explored in the real-time analysis of biomolecules due to their biocompatibility, non-toxic properties, and low costs. Different types of carbon materials, such as single-walled CNTs, multi-walled CNTs, graphene, and reduced graphene oxide (rGO) have been exploited for biosensing and electrochemical sensing applications [22,23]. CNTs exhibit both metallic and semiconductor properties, depending upon the diameter, chirality, and number of sheets of the tubes. Arc discharge, laser ablation, and chemical vapor deposition are the major methods for the growth of CNTs. Among the carbon-based nanomaterials, CNTs have been extensively explored in the development of electrochemical sensors due to their high surface-to-volume ratio, rapid electrode kinetics, and high conductivity [24,25]. Another widely studied carbon-based material is graphene, which is a two-dimensional carbon material with its carbon atoms arranged in hexagonal fashion. This novel carbon material exhibits good electrochemical, thermal, mechanical, and optical properties, which are desirable for designing a high-performance sensor platform. Various carbon nanomaterials-based electrochemical sensors and biosensors has been reported for pharmaceutical, environmental, and biomedical applications [26–31]. The advantages of using a nanomaterials-based approach for electrochemical sensing are the improved selectivity, reduction of cost, potential for miniaturization, and higher sensitivity. Detecting neurotransmitters using a bare electrode could be challenging due to its low sensitivity and selectivity. Nanomaterials-based electrochemical sensors provide distinct advantages over those without nanomaterials.

Broad scientific knowledge and modern engineering have led to the design and development of miniaturized and portable electrochemical sensors and biosensors for the *in vitro* and *in vivo* detection of neurotransmitters. Nanomaterials-based electrochemical sensors have increasingly appealed to researchers in the disciplines of analytical chemistry due to their augmented electrocatalytic activity, high surface area-to-volume ratios, and possible functionalization enabling them with tailor-made physicochemical properties. Over the last decade, nanomaterials-based electrochemical sensor and biosensors emerged as a promising strategy for the detection of neurotransmitters with improved selectivity and sensitivity [32–34]. This review will strive to elucidate the recent development of nanomaterials-based electrochemical sensors for the *in vitro* and *in vivo* detection of common neurotransmitters, including epinephrine, dopamine, serotonin, norepinephrine, glutamate, acetylcholine, nitric oxide, and purines. Besides the *in vitro* detection, this review also highlights some recent *in vivo* monitoring of neurotransmitters in the live tissues of drosophila, rats, chicken, and zebrafish. Some core issues associated with the electrochemical approaches used in the detection and monitoring of neurotransmitters and the future development in this exciting area are addressed.

2. In Vitro Detection of Typical Neurotransmitters

The introduction of the electrochemical techniques in neurochemical detection has created some significant advantages, such as portability, rapid response, low cost, and self-contained instrumentation. In this section, the recent advancements in the nanomaterials-based *in vitro* electrochemical analysis of the aforementioned common neurotransmitters is presented.

Epinephrine (EP), which is also known as adrenaline, is a catecholamine neurotransmitter. It increases the amount of glucose in the circulation via an enzymatic reaction to assist with fight or flight responses. The function of EP depends on its oxidation by an enzyme called amine oxidase, and its abnormal levels affect the regulation of blood pressure, heart rate, lipolysis, the immune system, and glycogen metabolism [33]. Parkinson's disease patients may have low amounts of EP in their bodies. In addition, EP has a positive impact on local sedative adsorption into the blood stream by narrowing the blood vessels, reducing toxic side effects, and increasing the duration of medicinal activity [34,35]. Nanomaterials-based electrochemical sensors show high performance in the detection of EP in a wide range of concentrations. As shown in Figure 2, DPV and amperometry were employed to detect EP using a nanoporous sponge-like Au–Ag electrode, showing a systematic increase in the current density in the concentration range of 10–275 μM and 25–500 μM , respectively [36]. In the DPV method, the highest sensitivity ($1.52 \text{ mA cm}^{-2} \text{ mM}^{-1}$) and the lowest detection limit

(5.05×10^{-6} M) were observed for the efficient detection of EP in the presence of ascorbic acid (AA). In contrast to bulk gold, this dealloyed nanoporous Au–Ag film showed high electrocatalytic activity for EP oxidation due to the nanosize effect of the electrode. As proposed in Figure 2C, the EP oxidation followed the electron transfer–chemical reaction–electron transfer (ECE) mechanism. The mechanisms of the electrochemical detection of neurotransmitters could be varied with the different neurotransmitters being investigated. In general, the loss of one or more electrons from the molecule leads to a change in functional groups, as well as a change in the molecule's structure. For example, in Figure 2, the first step of the oxidation of epinephrine involves the loss of two electrons and the formation of epinephrinequinone. The following step involves a further change of the structure to leucoadrenochrome via the formation of a five-membered ring. Wierzbicka et al. reported highly ordered gold/aluminum oxide as a sensing platform for the detection of EP, showing high sensitivity of $2.05 \text{ mA cm}^{-2} \text{ mM}^{-1}$ and the lowest detection limit (2.43×10^{-6} M) in the presence of uric acid (UA) [37]. Beitollahi et al. modified a glassy carbon electrode (GCE) with CNTs and 2-(4-oxo-3-phenyl-3,4-dihydro-quinazoliny)-*N'*-phenyl-hydra-zinecarbothioamide for the simultaneous determination of EP and norepinephrine (NE) [38], where two well-defined peaks with a separation of 240 mV appeared in the SWV. In another study, ZnO-based molecularly imprinted polymer arrays were employed to detect EP in the presence of UA and AA using DPV with a sensitivity of $0.66 \text{ } \mu\text{A } \mu\text{M}^{-1}$, which was lower than that of some previously discussed work. This may be ascribed to its low crystallinity and the high resistance of the fabricated non-noble metal oxide-based materials [39]. As the electrochemical oxidation of EP and dopamine may occur at a similar electrode potential, the design of the nanomaterials is crucial for the real sample analysis for the selective detection of EP. One strategy that can be employed to improve the selectivity of the electrode is to modify the surface with some chemical moieties (e.g., functional groups) that have a higher affinity to EP over dopamine.

Dopamine (DA) is a neurotransmitter of the phenethylamine family that participates in metabolism, attention span, central nerve function, emotions, and neuronal elasticity. It also regulates plasma glucose levels, endocrine function, and neuroimmune regulation [40–42]. The DA receptor in the peripheral nervous system activates DA, and the activated DA is involved in cross-talk between the immune and neural systems. An abnormal activated DA level may cause neuro-immune system dysfunctions [43–45]. Molecularly imprinted polymers on a gold electrode were employed for the detection of DA in human blood serum using DPV with the limit of detection of $0.13 \text{ } \mu\text{M}$ [46]. The designed electrode exhibited high selectivity, effectively discriminating DA molecules from AA and UA. Electrochemical detection with microchip electrophoresis is a novel approach for the analysis of neurotransmitters. A palladium microelectrode with microchip capillary electrophoresis was employed for the selective detection of DA with a sensitivity of $2.6 \text{ pA } \mu\text{M}$ and a detection limit of $2.1 \text{ } \mu\text{M}$. As palladium does not show high catalytic activity for the electrochemical oxidation of DA, the integration of platinum and/or gold with palladium was proposed to improve the performance of the palladium-based sensor [47]. Gold nanowires (Au NW), with different widths in the range of 30–1500 nm, were used for the oxidative detection of DA [48]. The current density of the Au NW electrode (25.87 mA cm^{-2} @ NW ~614 nm) was much higher than that of an Au thin film (0.043 mA cm^{-2}). However, the selectivity of the NW-based sensor needs to be improved for real sample tests. Core-shell and hollow poly(3,4-ethylenedioxythiophene)/poly(*N*-methylpyrrole)/poly(3,4-ethylenedioxythiophene) microspheres, fabricated using chemical polymerization with FeCl_3 , had the capacity to detect DA with a concentration range from 0.5 to 2 mM [49]. These polymer-based electrode materials showed efficacy as electrochemical sensors, and this approach may be used to fabricate various multilayered sensor platforms with dopants. As displayed in Figure 3, polymer-based organic electrochemical transistors (OECT) with graphene were demonstrated to have a limit of detection (LOD) of 5 nM for DA [50]. The mechanism of the electrochemical oxidation of dopamine involves a two-electron transfer to form dopamine-o-quinone. A magnetic Fe_3O_4 /rGO-based sensor has been reported for the

simultaneous detection of AA, DA, and UA using DPV [51]. A carbon nanorod array electrode was developed for the sensitive detection of dopamine with a limit of detection of 60 nM and a sensitivity of $7 \text{ nA } \mu\text{M}^{-1}$ [52]. Xinying et al. fabricated a graphene-based electrode to detect DA in the presence of a number of potential interferences such as EP, UA, and AA. Moreover, the DA in rabbit serum was also analyzed with a recovery of 97.8% [53]. A generator–collector approach was established for selective DA detection in the presence of AA using microwell arrays with the concept based on redox cycling. Under such experimental conditions, the interfering species is discriminated diffusionally. The analyte may freely diffuse into the microcavities and be involved in the electrochemical reactions. However, more theoretical and experimental findings are required to understand the detection mechanisms in the presence of other neurochemicals, especially EP and norepinephrine [54]. DA oxidation was conducted on the surface of multilayer graphene nanobelts/glassy carbon electrode using amperometry in the presence of potential interferences. The amperometry response of the graphene nanobelt exhibited a sensitivity of $0.95 \mu\text{A } \mu\text{M}^{-1}$ for the DA oxidation [55]. As shown in Figure 4, an electrochemically formed nickel oxide nanoparticle/multiwalled carbon nanotube (MWCNT) was tested for the simultaneous detection of neurochemicals, and the sensitivity of DA and EP were calculated to be 3.8 and $3.9 \mu\text{A } \mu\text{M}^{-1}$, respectively [56]. Further, the detection was attempted in real samples such as human cerebrospinal fluid, human serum, and lung fluid spiked with DA and EP. The experimental measurements revealed that the recovery percentage was in the range between ~97–106%.

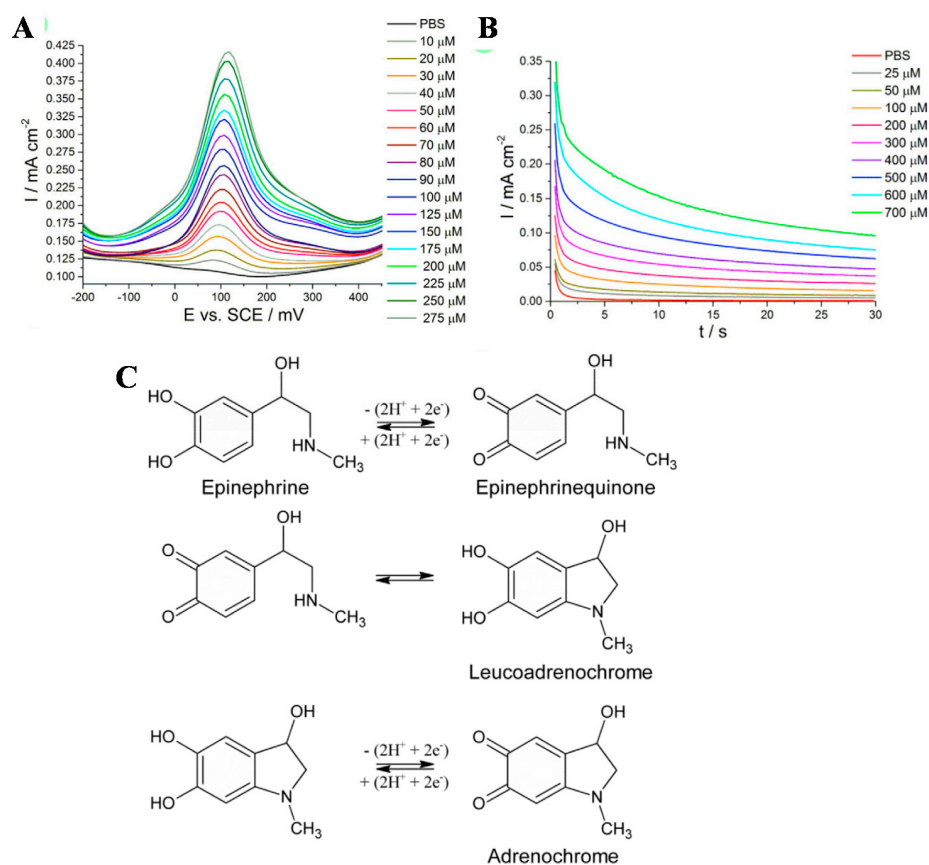


Figure 2. (A) Differential pulse voltammetry; (B) amperometry response of the nanoporous sponge-like Au–Ag electrode in 0.1 M PBS containing different concentrations of epinephrine (EP); (C) The electron transfer–chemical reaction–electron transfer reaction (ECE) mechanism of epinephrine electrochemical oxidation [36]. Copyright 2016, Springer.

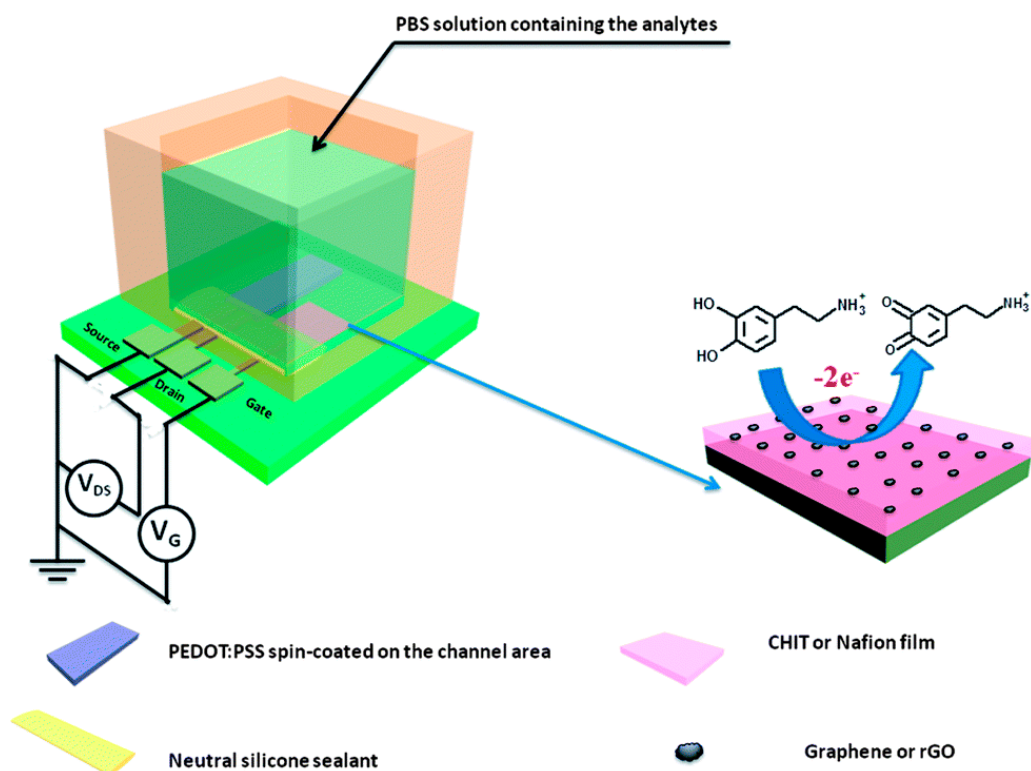


Figure 3. Schematic diagram of an OECT-based (organic electrochemical transistors) dopamine sensor modified with Nafion (CHIT) and graphene (rGO) flakes on the Pt gate electrode. The electro-oxidation of dopamine occurs on the surface of the gate (right figure) [50]. Copyright 2014, Royal Society of Chemistry.

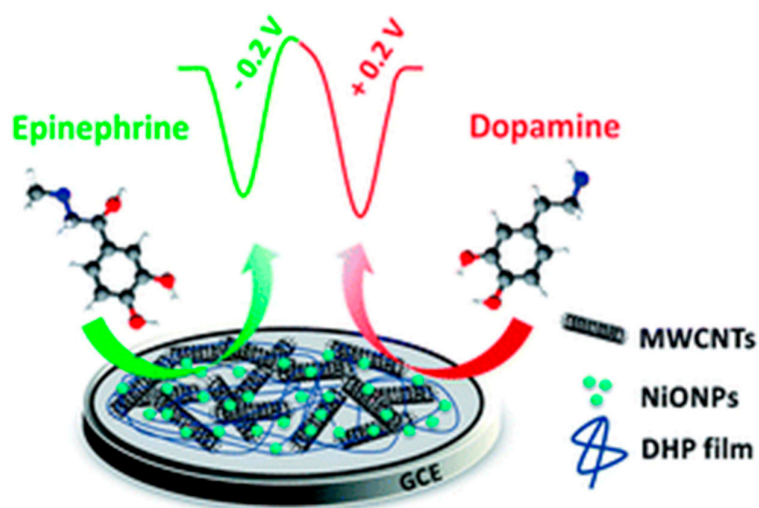


Figure 4. Schematic of the simultaneous detection of epinephrine and dopamine using multiwalled carbon nanotubes (MWCNTs) and dihexadecylphosphate (DHP) film [56]. Copyright 2014, Royal Society of Chemistry.

An organic field-effect transistor type (OFET) was developed using platinum nanoparticle-decorated rGO for the selective detection of dopamine in the presence of non-target molecules such as AA and UA, as well as tyrosine and phenethylamine [57]. Aside from nanomaterials-based sensors, an RNA-modified aptamer electrode was explored for the detection of DA in blood serum, as shown

in Figure 5. The sensitivity and LOD were $67 \pm 1 \text{ nA } \mu\text{M}^{-1} \text{ cm}^{-2}$ and 62 nM, respectively [58]. The positively charged cysteamine self-assembled monolayer (SAM) discriminated DA from the negatively charged interference molecules (e.g., AA) on the aptamer, which provided the selectivity to the fabricated sensors. In the DA detection, the potential interference of AA and UA may be avoided by the careful design of the electrode and the selection of materials [59]. However, interference from structurally related neurochemicals (e.g., DA and EP) is challenging to avoid. In such a case, receptor-incorporated nanomaterials-based sensing strategies need to be developed for the selective detection of DA.

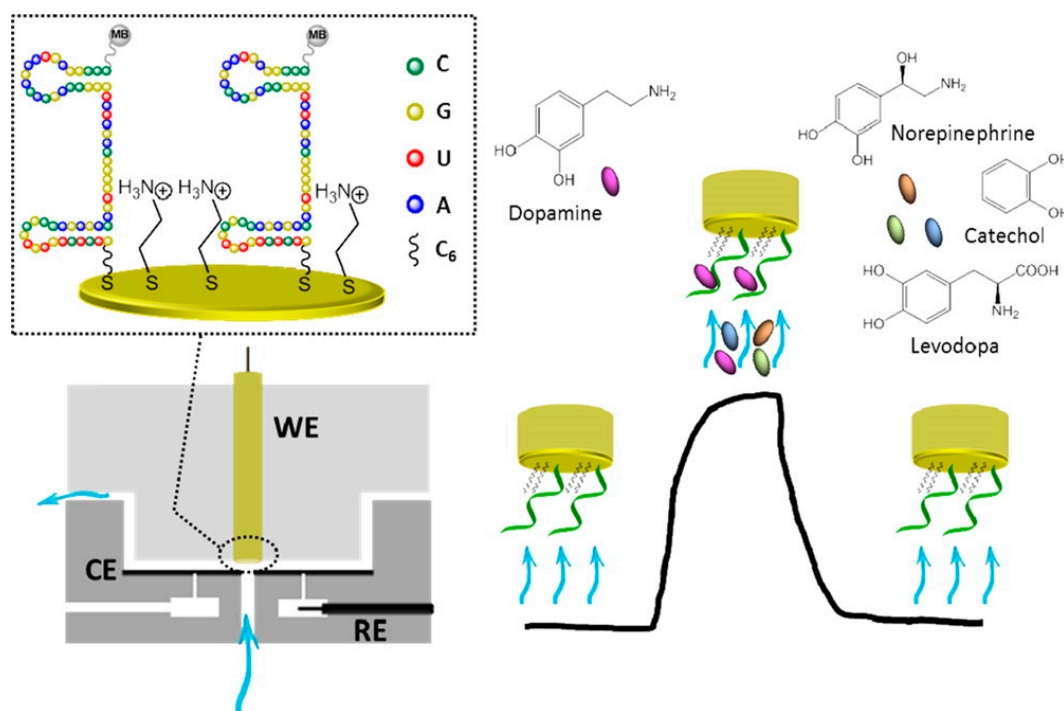


Figure 5. Schematic representation (left panel) of the flow-through wall-jet electrochemical cell (with a working electrode (WE), a counter electrode (CE), and an Ag/AgCl (0.1 M KCl) reference electrode (RE)) used for dopamine electroanalysis and the aptamer-modified gold electrode surface. The right panel image shows the chronoamperometric response of the aptasensor to dopamine, selectively trapped from the flow of neurotransmitters over the sensor surface. Following each measurement, the electrode surface was regenerated in a flow of a blank buffer solution to remove the oxidized analytes [58]. Copyright 2016, American Chemical Society.

Serotonin or 5-hydroxytryptamine (5-HT) is involved in many biological processes, including behavior and sensory perception. The concentration of 5-HT in the human brain is 10 mg, where 2% is present in the central nervous system. Changes in 5-HT concentrations create different neurological and psychiatric issues. Further, 5-HT levels are directly related to gastrointestinal illness [60]. For all the above reasons, the detection of 5-HT has great significance in the diagnosis of various diseases and in elucidating its role in several neurological disorders. As low 5-HT levels in the brain may be an indicator of depression, its presence in the blood, serum, plasma, and platelets may be considered as a peripheral biochemical marker for depression [60]. The oxidation of 5-HT involves the transfer of two electrons to form serotonin quinoneimine. Cesarino et al. fabricated an electrode with platinum nanoparticles/polypyrrole/MWCNT/silver nanoparticles for the detection of 5-HT and achieved a detection limit of $0.15 \mu\text{M}$ using DPV [61]. The synergistic effect of the nanohybrid was responsible for the sensitive detection of 5-HT. As in the abovementioned work, gold/polypyrrole nanocomposites were developed for the detection of 5-HT and revealed high sensitivity ($0.3316 \mu\text{A} \cdot \mu\text{M}^{-1}$) and a low

detection limit of 33.22 nM [62]. The polymer-incorporated sensing platform assisted to control the accumulation of 5-HT on the electrode surface for high performance. However, a high concentration of glucose significantly affected the 5-HT signal by about 30%. Based on Fe₃O₄-MWCNT-poly (bromocresol green) film, the electrochemical detection of 5-HT was also achieved using DPV, and it permitted detection in the concentration range between 0.5 and 100 μM with a detection limit of 0.08 μM [63]. The interference of UA oxidation significantly limited the sensing performance of the electrode for 5-HT when the UA concentration increased by 20-fold. A polyethylenimine CNT fiber microelectrode (PEI-CNT MEs) was employed for the oxidation of 5-HT, and a comparison of its performance with a carbon-fiber microelectrode (CFMEs) is shown in Figure 6. The PEI-CNT MEs showed high selectivity and a stable response compared with CFMEs. The biofouling by serotonin and its metabolite interferant 5-hydroxyindoleacetic acid (5-HIAA) decreased the current response to 50% for CFMEs, whereas no significant current drop was observed with respect to PEI-CNT MEs (retains 100%) [64]. Thus, these PEI-CNT MEs may be beneficial for the real-time analysis of 5-HT. The detection of 5-HT can be improved through the incorporation of a selective ion exchange resin capable of repelling interfering molecules.

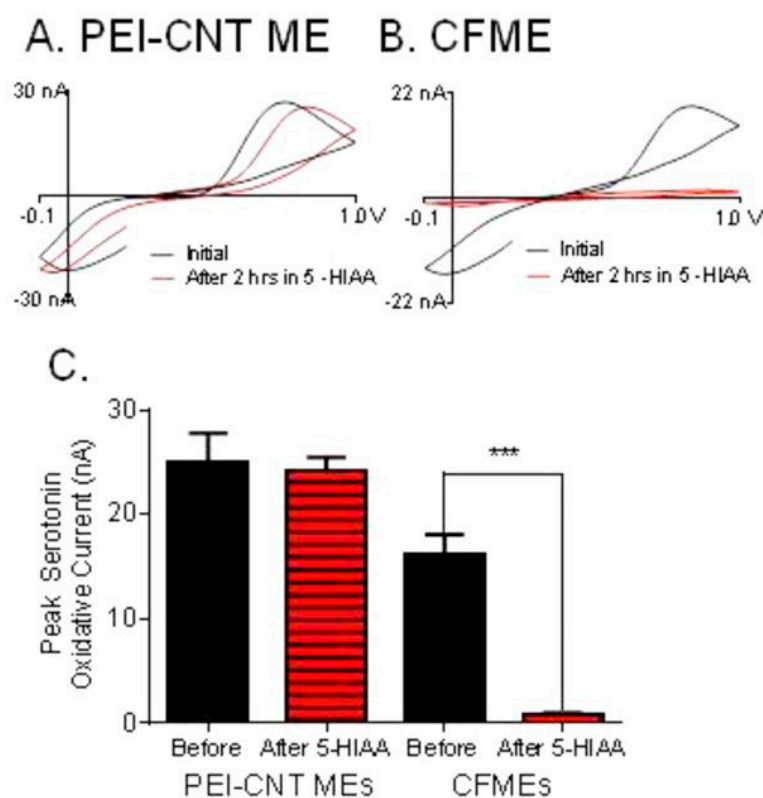


Figure 6. 5-hydroxyindoleacetic acid (5-HIAA) fouling in vitro. One micromolar serotonin was detected at a polyethylenimine CNT (PEI-CNT) fiber electrode before and 2 h after it was bathed in 10 μM 5-HIAA, while the waveform was applied. The applied waveform was the serotonin waveform (0.2–1.0 to −0.1 to 0.2 at 1000 V·s^{−1}). (A) The cyclic voltammograms (CVs) are similar before and after 5-HIAA at the PEICNT microelectrodes; (B) For carbon-fiber microelectrodes (CFMEs) after 2 h in 10 μM 5-HIAA, the oxidation peak of serotonin was no longer visible; (C) Bar graphs depicting the change in peak oxidative current for serotonin prior to and following exposure to 10 μM 5-HIAA for 2 h [64]. Copyright 2014, American Chemical Society.

Norepinephrine (NE) is involved in the elevation of heart rate, blood pressure, pupil dilation, airway dilation, and the constriction of blood vessels. It also participates in glycogen metabolism

and plays a major role in the sleep–wake cycle, attention, focus, learning, and memory [65]. Despite the significant volume of robust mechanistic and clinical trial data supporting the benefits of the renin–angiotensin–aldosterone system and the beta-adrenergic receptor blockade in adults with systolic heart failure, it remains unclear whether these mechanisms are also involved in mediating heart failure in single-ventricle patients [66]. Without such knowledge, further clinical trials of neurohormonal blockades in single-ventricle patients will remain unappealing [67,68]. The oxidation of norepinephrine is similar to that of epinephrine, as illustrated in Figure 2C, where a two-electron transfer takes place to form norepinephrine quinone. Hydrothermally prepared MoO₃ nanowires deposited on GCEs showed an improved response for the oxidation of NE with a response time of 2 s and detection limit of 0.11 μM [69]. From the CV curves, the heterogeneous electron transfer rate constant was calculated to be $8.03 \times 10^{-4} \text{ cm s}^{-1}$. The improved electrochemical performance was attributed to the high catalytic activity and one-dimensional (1D) microstructure of the MoO₃ nanowires, which allowed for easier electron transport and increased the overall performance of the sensor. In addition, nanorod-shaped FeMoO₄ was investigated for the electrochemical detection of NE, and the LOD was determined to be 3.7 nM. These 1D non-noble metal-based nanostructures exhibited high sensing performance similar to enzyme- and noble metal-based electrochemical sensors [70]. Moreover, the electrochemical oxidation of NE was demonstrated on carbon paste electrodes with carbon nanotubes (CNT-CPE) and a molybdenum (vi) complex, which facilitated the electron transfer of NE at the surface of the electrode, which led to the non-interferent detection of NE with a LOD of $0.039 \mu\text{A} \cdot \mu\text{M}^{-1}$ [71]. The simultaneous detection of NE and acetaminophen was proposed using MnO₂-decorated rGO. The proposed MoO₂-rGO simultaneously detected the NE and acetaminophen with detection limits of 2.0 nM and 0.4 μM, respectively [72]. Screen-printed mesoporous carbon was utilized for the oxidation of NE, and the LOD was determined to be 0.589 nM using the amperometry technique [73]. The performance of the sensor is directly related to the -surface area of the mesoporous carbon. Further, various metal and/or metal oxide-decorated carbon-based nanocomposites have been utilized for the detection of NE in the presence of other neurochemicals [74,75]. However, the selective detection of NE is still a challenging task due to the mutual interference of other neurotransmitters, especially in the presence of EP and DA. Again, the use of a selective resin, ion channel, or functional groups could be a viable strategy to achieve higher selectivity for the detection of NE, as well as EP and DA.

L-Glutamate (L-Glu) is an excitatory transmitter in the vertebrate brain that is expressed in glial cells, behaves as potential neurotoxin by its overstimulation of its membrane receptors, and participates in the synthesis of the glutathione antioxidant [76]. Signal processing in the retina is controlled via the integration of excitatory and inhibitory inputs of retinal neurons [77,78]. The distribution of glutamate receptor “subtype” retinal neurons has been characterized by immunohistochemical techniques [79]. The oxidation of L-Glu involves an oxidative deamination in which the amine group on the second carbon is converted to a carbonyl group. This two-electron transfer forms α-ketoglutarate as the product. A multisite array of two microelectrodes on a ceramic base was fabricated to detect L-Glu using glutamate oxidase, where the low detection limits (0.98 μM) and excellent linear range from 0 to 200 μM were observed for the in vitro analysis of L-Glu [80]. This approach was also useful for glucose detection. A ferrocene-incorporated single wall carbon nanotube (SWCNT) was investigated for the oxidation of L-Glu using CV and amperometry techniques. The ferrocene/SWCNT exhibited a fast response to attain dynamic equilibrium for each addition of L-Glu from 1 to 7 μM and generated a steady-state current in amperometry [81]. Dorozhko et al. conducted L-Glu oxidation using a carbon-containing electrode modified with gold (CCEMG) and showed an analytical signal for L-Glu with linear behavior in the range from 3.2×10^{-4} to 2.5×10^{-3} M. This enzyme-free detection method revealed that the potential of the L-Glu oxidation peak was dependent upon the pH [82]. The enzymatic electrochemical detection of L-Glu was performed through the immobilization of glutamate oxidase (Gluox) onto a carboxylated MWCNT/gold nanoparticle/chitosan complex film modified on a gold electrode. The optimal response time of the fabricated biosensors was 2 s with a high sensitivity ($155 \text{ nA} \cdot \mu\text{M}^{-1} \cdot \text{cm}^{-2}$) and low detection limit (1.6 μM). Further, this biosensor

showed no potential interference with other biomolecules that were present in blood serum under physiological conditions [83]. However, these enzymatic biosensors often suffered poor stability, low conductivity, and the blockage of catalytic sites. To overcome this issue, the design of functional nanomaterials and electrochemical biosensors needs to be further improved. For instance, core-shell alloys and multi-dimensional nanocomposites may be designed to enhance the electron transfer rate and durability of the biosensors.

Nitric oxide (NO) is a gaseous neurotransmitter that is synthesized by three isoforms of nitric oxide synthase (NOS): NOS-I (neuronal NOS), NOS-II (cytokine inducible NOS), or NOS-III (endothelial NOS) [84]. Neuronal NO diffuses through cell membranes and functions as a neuromodulator in the brain. It is involved in various behaviors as it interacts with many signaling pathways [85]. The electrochemical oxidation of NO may result in nitrite (NO_2^-) and nitrate (NO_3^-). A copper (II) chlorophyllin-zinc oxide screen-printed electrode was used for the detection of NO with a wide linear range of concentration from 200 to 1 mM. The sensor exhibited sensitivity of $96.4 \text{ nA} \cdot \mu\text{M}^{-1}$ with a LOD of 100 nM. This electrode also assisted with the detection of NO metabolites, such as NO_2^- and NO_3^- , in human serum samples prior to and following the introduction of a beet root supplement [86]. An investigation into the electrochemical oxidation of NO was conducted using platinum–tungsten nanoparticles, rGO, and an ionic liquid (IL), where a sharp peak for the NO oxidation was observed at a potential of 0.78 V versus Ag/AgCl with CV and DPV [87]. As shown in Figure 7, the proposed electrochemical sensor exhibited high stability with a low LOD (0.13 nM) and high sensitivity ($3.01 \mu\text{A} \cdot \mu\text{M}^{-1} \text{ cm}^2$). The sensor was investigated in real samples such as human serum and urine samples and demonstrated exclusive selectivity towards NO [87]. Gold/platinum/reduced graphene oxide was utilized for NO detection, which exhibited a high sensitivity of $7.35 \mu\text{A} \cdot \mu\text{M}^{-1}$ and a LOD of 2.88 nM with negligible interference from other organic molecules [88]. The noble metal-based nanocomposite was then tested to monitor the release of NO in cardiac cells. Amperometry was employed to exploit the detection of NO in cardiac and cancer cells using a hierarchical nanoporous gold (HNG) electrode, where Figure 8 details NO sensing in live cells [89]. This HNG electrode provided an effective platform for monitoring NO in biological processes and in bioreactors. The nitrite anion may affect the selectivity of the sensors because it is the main interference molecule, and its oxidation occurs close to the NO oxidation potential. In addition, these NO oxidations are typically held at higher over potentials, so the amperometric technique may not be suitable for NO sensing in the presence of other neurotransmitters. However, dialysis and/or electrophoresis coupled with amperometric techniques may be utilized for real sample testing. The miniaturization of these sensors is desirable for the in vivo electrochemical detection of NO.

Acetylcholine (ACh) is a well-known neurotransmitter that mediates the chemical transmission of neural signals. ACh signaling in the synapses of the central and peripheral nervous system regulate most biological and physiological functions, such as ligand-gated ion channels and bursting mode neuronal firing. Imbalances of ACh in both the central and peripheral nervous systems are associated with different health issues such as Parkinson's disease, Alzheimer's disease, and myasthenia gravis [90]. Ca^{2+} -induced ACh from leukemic cells could be monitored electrochemically, which may lead to the development of detection kits for Alzheimer's and Parkinson's diseases. In addition, variations in the levels of ACh disrupts behavior, learning, and sleep [91,92]. In the electrochemical oxidation of ACh, two-electron transfer is involved and leads to choline and acetate as byproducts. An Au self-assembled monolayer surface was investigated for the acetylcholinesterase (AChE) activity assay and its inhibitors using electrochemical oxidation. The generated *o*-Quinones were used as redox probes [93]. AChE and choline oxidase (ChO) enzymes were covalently bound to a chitosan/gold/ferric oxide nanocomposite. At a pH of 7.0 and 30 °C, the ChO hydrolyzed ACh and generated H_2O_2 , which was indirectly detected using amperometry with an optimal response time at 3 s, with a working linear range from 0.005 to 400 μM and detection limit of 0.005 μM for ACh. This electrode was tested using the blood serum of normal and Alzheimer's patients [94]. The enzyme-coated electrode lost 50% of its initial activity over a period of 3 months. Furthermore,

AChE-MWCNT-Fe₃O₄ nanoparticles-chitosan was demonstrated for the rapid detection of ACh. The fabricated electrode exhibited pH- and temperature-dependent sensing performance with a LOD of 0.6 nM [95]. The detection of ACh was also done using AChE–ChO immobilized polypyrrole-polyvinylsulphonate-based enzymatic electrodes, where the detection limit of the sensor was 5.0 nM. In addition, the storage and operational stability were studied for 18 continuous assays and retained an 83.1% current response. The sensitivity of the developed sensor decreased with the increasing of the film thickness and the increasing of the enzyme concentration, because the film thickness and enzyme concentration were proportional to the conductivity of the modified films [96]. The analysis of neurotransmitters requires that the detection limit be low enough to measure the smallest concentration that might exist in an organism, as well as a linear range that encapsulates the typical concentrations that exist in the organism in question. This means that a lower detection limit and a wide linear range are the most beneficial when comparing different nanomaterials. The disparity between the linear range and the detection limit of different nanomaterials may be due to the rate at which the electron transfer takes place, the accessibility of the neurotransmitter on the electrode surface (i.e., whether or not more molecules can travel into the surface to allow for more oxidation events), or the affinity of the neurotransmitter to the electrode surface. In addition, different applied potentials may be required for different nanomaterials, as seen in Table 1. Overall, ACh detection was performed based on the sensing of enzymatically produced hydrogen peroxide (H₂O₂). Most of the reported biosensors for ACh involved multiple steps for the immobilization and functionalization of the electrodes, which are time consuming and tedious processes. Moreover, the stability of the biosensors was limited due to the enzyme immobilization, which is sensitive to pH and temperature. Therefore, enzyme-free nanomaterials-based electrochemical sensors need to be explored for the detection of ACh with high sensitivity, high stability, and a stable response.

Purines or adenosine 5'-triphosphate (ATP) is an important neurotransmitter, which is present in peripheral tissues and serves as a neurotransmitter and neuromodulator in the perivascular nerves. It has a role in physiological and pathophysiological factors such as the age, type, species, size, tone, pressure, and temperature of the blood vessels. It also combines with NE to become a predominant neurotransmitter at high blood pressures [97]. The oxidation of ATP follows a simple cleavage of the bond between the phosphorous and oxygen of the phosphate groups. This cleavage releases two electrons to form adenosine 5'-diphosphate (ADP). A target-responsive electrochemical aptamer switch (TREAS) was functionalized on a gold surface that was dually labeled with 3'-SH and 5' ferrocene for the detection of ATP among guanosine triphosphate, cytidine triphosphate, and uridine triphosphate interferences. In SWV, the peak current increased only with the addition of ATP (10–1 mM) at a potential of 0.26 V [98]. The simultaneous quantification of potassium ions and ATP was carried out using a nanochannel-based electrochemical method. A Pt-porous aluminum analog of ion channels detected the concentrations of K⁺ and ATP in the ranges of 0.05–10.0 mM and 0.0005–1.0 mM, respectively. The selectivity and stability of these nanochannels were not altered for up to 4 cycles [99]. A direct method for the detection of ATP was demonstrated using a paper-based system. Chemically prepared graphene was loaded onto mixed cellulose ester filter paper. After five minutes, the membrane was vacuum filtered to assemble the graphene, and the excess was rinsed away. Subsequently, these electrodes were dried and employed for the oxidation of ATP. Cellular ATP analysis was conducted using K562 leukemia cells, human adenocarcinoma HeLa cells, and normal human breast cells. In DPV, the ATP was detected at a potential of 1.34 V, and the observed linear range was from 0.3 to 450 μM with a detection limit of 0.08 μM. The oxidation of ATP resulted in irreversible byproducts being adsorbed on the sensing platform and the reduction of the sensitivity and reproducibility of the sensors [100]. The biofouling of these electrodes is a major concern and a target for the improvement of these sensors. The functionalization of the surface with a material that has a lower binding energy for the fouling agent could aid in the release of the formed intermediates and products. One approach might be the incorporation of core-shell alloy nanoparticles with a low binding energy for biofouling products.

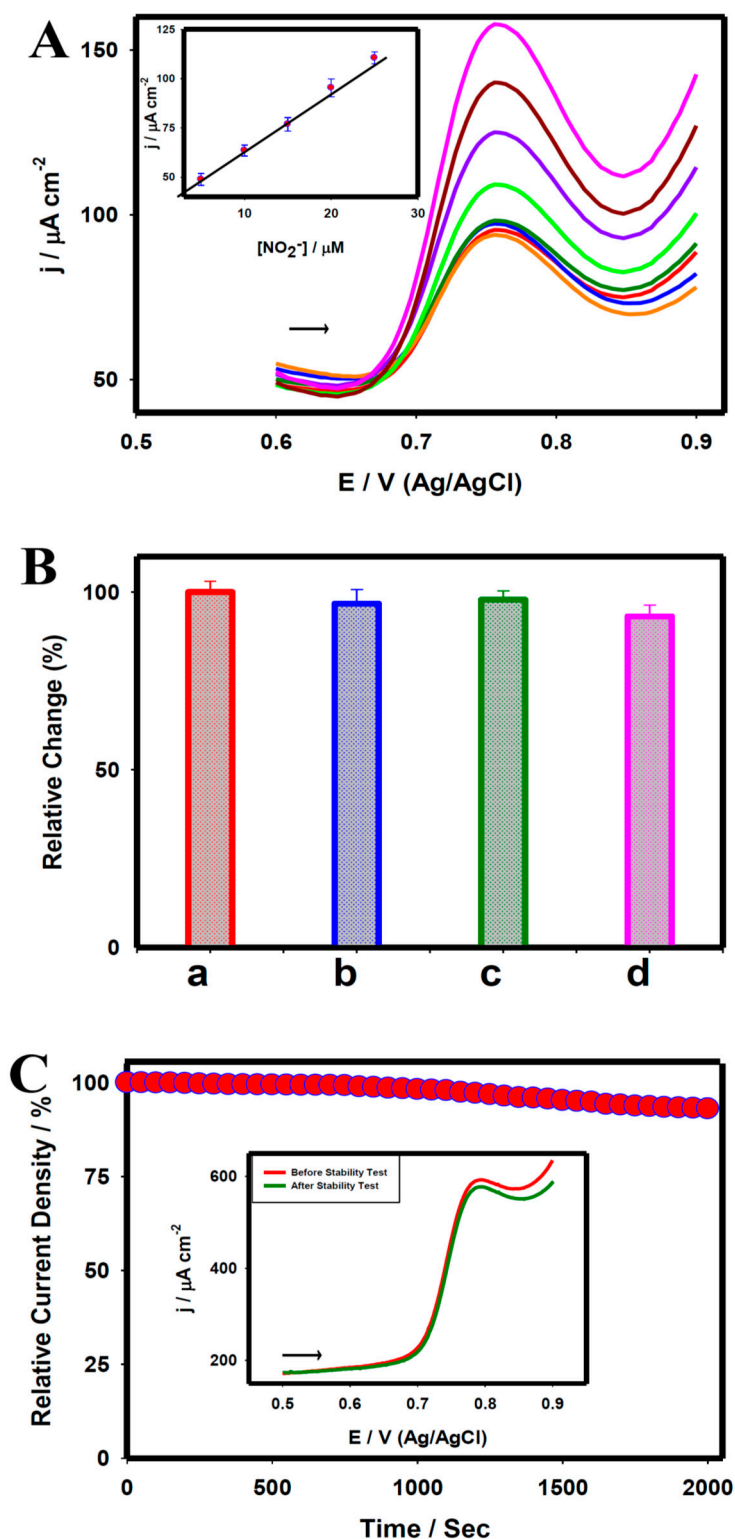


Figure 7. (A) Differential pulse voltammograms (DPVs) recorded for the PtW/rGO-IL nanocomposite electrode in 5 μM of NO_2^- (red) and a mixture with 50 μM of dopamine (DA, blue), DA + ascorbic acid (AA, dark green), DA + AA + uric acid (UA pink), and 10 (green), 15 (purple), 20 (brown) and 25 μM of NO_2^- (pink). Inset: The corresponding calibration plot; (B) The plot of the relative response of 5 μM of NO_2^- (a) and mixture with 50 μM of DA (b), DA + AA (c), DA + AA + UA (d); (C) Amperometric responses of the PtW/rGO-IL nanocomposite electrode recorded in 1 mM of NO_2^- (E_{app} :0.78 V). Inset: linear sweep voltammograms (LSVs) recorded the PtW/ rGO-IL nanocomposite electrode prior to and following the stability tests in 1 mM of NO_2^- [87]. Copyright 2016, Springer.

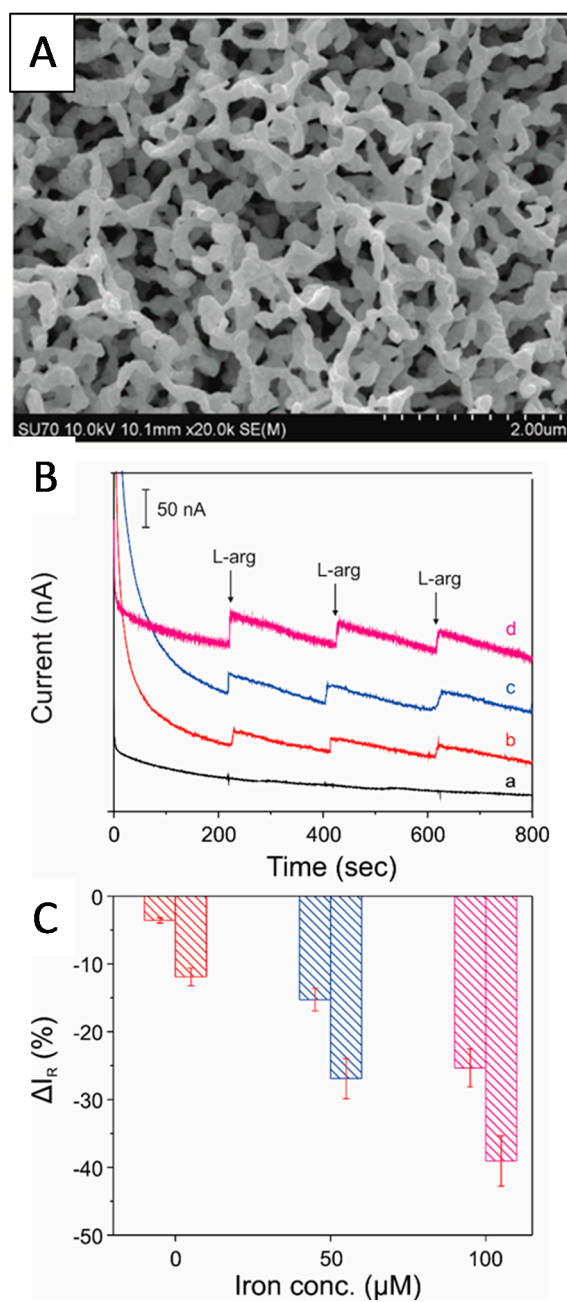


Figure 8. (A) SEM images of the hierarchical nanoporous gold (HNG) microwire treated by electrochemical alloying/dealloying in a mixed electrolyte of benzyl alcohol (BA) and ZnCl_2 . (B) Amperometric responses to nitric oxide (NO) released from cardiac cells with the successive addition of L-arginine in a 0.1 M of PBS solution (a), containing cultured cells (b), or cultured cells treated with 50 μM of iron (c) or 100 μM of iron (d). Applied potential: 0.80 V. (C) The decreased percentage of the responses of NO in comparison with that obtained following the first injection of L-arginine, respectively [89]. Copyright 2017, American Chemical Society.

Table 1. A list of nanomaterials-based sensing platforms and their performances in the detection of neurotransmitters.

Neuro-Transmitters	EC Method	Nanomaterials	E/(V vs. RHE)	Interferent	Linear Range (μM)	LOD (μM)	Ref
EP	DPV	MWCNT-PANI-TiO ₂	0.821	5-HT and AA	4.9–76.9	0.160	[101]
	DPV	Polypyrrole nanotubes/Gold nanoparticles	0.914	Glucose, D-fructose, citric acid, UA, AA, DA	35–960	0.298	[102]
	CV	Graphene	0.655 *	AA and UA	1–1000	0.24	[103]
	DPV	MWCNT	0.782	AA	7.5–48	4.6	[104]
	CV	TX 100-modified carbon paste electrode	0.810	AA and FA	10–50	1.0	[105]
DA	DPV	2D-hexagonal boron nitride	0.862	AA and UA	3–75	0.65	[42]
	DPV	Carbon dots	0.885	AA and UA	0.01–30	0.01	[106]
	AP	Pt ₃ Ni nanoalloys	0.922	Glucose, AA, and UA	0.5–250	0.01	[107]
	AP	Multilayer graphene nanobelts	0.81	Hydrazine, UA, AA, lactic acid, glucose	2–20	0.58	[55]
	CV	Multilayered hollow sphere	0.922	None	0.5–2	0.5	[49]
5-HT	DPV	Carbon nanofiber	0.910	AA	0.001–1000	0.001	[108]
	DPV	WO ₃ nanoparticles	0.985	AA, EP, DA, UA, FA, Glucose	0.01–600	0.001	[109]
	SWV	MWCNT/ZnO	0.920	AA and UA	0.05–1	0.01	[110]
	DPV	Poly (bromocresol green)/Fe ₃ O ₄	0.985	AA, UA, and DA	0.2–100	0.060	[63]
	SWV	GCE-MWCNT-NiO	0.980	DA and AA	5.98×10^{-3} –62.8	0.118	[111]
NE	AP	FeMoO ₄	0.952	UA and AA	0.05–200	0.003	[70]
	SWV	CTAB-SnO ₂	0.822	EP	0.1–300	0.006	[112]
	SWV	MWCNT/ZnO	0.704	AA and UA	0.5–30	0.2	[104]
	CV	Pd nanoparticles	0.862	AA, UA, and FA	0.5–80	0.1	[113]
	AP	MoO ₃ Nanowires	1.01	AA, UA, L-Glu, NH ₄ ⁺ , K ⁺ , DA, Na ⁺ , Fe ³⁺ , Cl ⁻	0.1–200	0.11	[69]
L-Glu	CV	GCE/gold	-0.061	None	320–2500	0.40	[82]
	AP	Co ₃ O ₄ /graphene/chitosan/GluOx	1.31	None	4–600	2.0	[114]
	CV	PpyNPs/PANI/AuE	0.440	Citric acid, AA, cysteine, methionine, lysine, aspartic acid, glucose, NaCl, glycine	0.02–400	0.1×10^{-3}	[115]
	AP	IrOx	-0.078	DA and AA	5–300	0.32	[116]
	CV	GluOx/cMWCNT/AuNP/CHIT	0.769	AA, bilirubin, urea, UA, triglycerides, glucose	5–500	1.60	[83]
NO	AP	PtW/rGO-IL	1.40	None	0.002–1200	0.13	[87]
	AP	Nanoporous Pt	1.37	None	0.0–8.75	0.001	[117]
	AP	Pt/MWCNT	0.190 *	None	0.40–0.10	0.10	[118]
	DPV	Au-Pt/rGO	1.35	NO ₂ ⁻ , NO ₃ ⁻ , cysteine, AA, and UA	0.02–10.0	0.003	[88]
	AP	Gold nanoporous microelectrode	1.42	AA, UA, cysteine, arginine	0.005–200	0.001	[89]
ACh	AP	AChE-ChO/PPy-PVS	1.03	AA, UA, EtOH, MeOH, paracetamol, cystine, cysteine, glucose	0.01–0.1	0.005	[96]
	CV	Chitosan/gold-coated Fe ₃ O ₄	0.86	None	0.005–400	0.005	[94]
	AP	Carbon fiber/AChE	0.584	None	0.3–100	1	[119]
	AP	Nickel oxide	1.11	None	0.25–5.88	26.7	[120]
	SWV	AChE/Hpg/Pt	0.910	None	240–1900	10	[121]

Table 1. Cont.

Neuro-Transmitters	EC Method	Nanomaterials	E/(V vs. RHE)		Interferent	Linear Range (μM)	LOD (μM)	Ref
Purines	DPV	B-doped CNTs	1.57 **	None		0.5–8	0.03	[122]
	EIS	Amino-functionalized MOF	OCP	AMP, GTP, ADP, IgP		0.001–1000	0.005	[123]
	CV	SWNTs	0.260	None		10–120	10	[124]
	CV	Graphene/AuNPs	0.210	None		1.14×10^{-4} –31	2.01×10^{-5}	[125]
	AP	Hemin/GO nanosheets	0.636	CTP, UTP, GTP, ADP, AMP		0.5×10^{-3} –0.1	0.08×10^{-3}	[126]

* Indicates that the reduction peak was used to detect the neurotransmitter. ** Adenosine was detected in this case, while all others in the purine section are ATP. EC—electrochemical; E—peak potential; V—volts; RHE—reversible hydrogen electrode; LOD—limit of detection; DPV—differential pulse voltammetry; CV—cyclic voltammetry; AP—amperometry; SWV—squarewave voltammetry, LSV—linear sweep voltammetry; EIS—electrochemical impedance spectroscopy; EP—epinephrine; DA—dopamine; 5-HT—serotonin; NE—norepinephrine; L-Glu—L-glutamate; NO—nitric oxide; ACh—acetylcholine; MWCNT/PANI/TiO₂—Multiwalled carbon nanotubes/polyaniline/titanium dioxide; MWCNT—multiwalled carbon nanotubes; 2D—two dimensional; GCE—glassy carbon electrode; FA—Folic acid; CTAB—cetyltrimethylammonium bromide; FTO—fluorine-doped tin oxide; rGO—reduced graphene oxide; IL—ionic liquids; PpyNPs/PANI/AuE—polypyrrole nanoparticles/polyaniline-modified gold electrode; GluOx/cMWCNT/AuNP/CHIT—glutamate oxidase/carboxylated multiwalled carbon nanotubes/gold nanoparticles/chitosan; AChE-ChO/PPy-PVS—acetylcholinesterase-choline oxidase/polypyrrole/polyvinylsulphonate; MeOH—methanol; EtOH—ethanol; GluOx—glutamate oxidase; AChE/Hpg/Pt—acetylcholine esterase/highly porous gold/platinum; MOF—metal organic framework; OCP—open circuit potential; SWNT—single walled nanotubes; AMP—adenosine monophosphate; GTP—guanine triphosphate; ADP—adenosine diphosphate; IgP—imidazole glycerol phosphate; ATP—adenosine triphosphate; GO—graphene oxide; CTP—cytidine triphosphate; and UTP—uridine triphosphate.

For in vitro analysis, various nanomaterials-based electrochemical sensors and biosensors have been reported for the measurement of EP, DP, NE, ACh, L-Glu, NO, and ATP, as listed in Table 1. The developed electrochemical sensors and biosensors showed efficacy in detecting the neurochemicals either individually or in the presence of multiple neurotransmitters. In general, multiple neurotransmitters were discriminated by enzyme-modified nanomaterials-based electrodes. In addition, nanoengineering of sensing platforms with separation techniques, such as micro dialysis, have been demonstrated for the selective detection of neurotransmitters. A difficult challenge to overcome is the biofouling of the electrode surface, and it significantly decreases the sensitivity and stability of the sensors. Future research may focus on the functionalization of nanomaterials to retard the accumulation of byproducts on the electrode. The selective detection of structurally related neurochemicals is challenging, and further development is required in nanomaterials-based electrochemical sensors. The toxicity analysis of nanomaterials and neurochemical oxidation byproducts are required for the use of the nanomaterials-based electrochemical sensors in direct clinical applications.

3. In Vivo Analysis of Neurotransmitters

The in vivo electrochemical analysis of neurotransmitters can elucidate their real-time functionality in the brain and body. This type of analysis might be very useful for the monitoring, control, and potential manipulation of chemical changes that occur as the result of different diseases and to facilitate the diagnoses of diseases at their early stages. In this section, we describe the in vivo analysis of neurotransmitters in several live organisms, such as the chicken, fruit fly, and rat.

The chick is often being used for in vivo analysis to provide prototype information of the brain and its functions. Raquel et al. attempted to simultaneously detect EP and NE levels in chick brains using high-performance liquid chromatography coupled with a coulometric detection method. This study revealed the role of neurotransmitters during the first day after hatching. The EP and NE presence in the cerebellum in different stages were monitored from the late embryonic period to the post-hatching period [127].

A carbon nanopipette electrode (CNPE) was employed to detect the presence of DA in *Drosophila melanogaster* (fruit fly) [128]. The diameter of the tip was approximately 250 nm and exposed to different concentrations of DA under in vitro conditions. Subsequently, this electrode was used to detect the endogenous DA release in *Drosophila* larvae, which confirmed that the CNPEs could be used for in vivo neuroscience investigations and inspired researchers to develop sensor implants for the localized measurement of neurotransmitters. These CNPEs are tunable with different dimensions, which may facilitate the implantation and monitoring of neurotransmitters in a small organism (e.g., *Drosophila*). The carbon-fiber microelectrode was employed to measure the DA and 5-HT in freely moving rats using DPV with wireless technologies [129]. In these technologies, Nafion-coated micro biosensors were surgically affixed within the prefrontal cortex in the brains of the rats; the sensors were activated to record signals that indicated the presence of DA and 5-HT. Moreover, a wearable, wireless, electrochemical instrument was developed for the detection of DA. A carbon-fiber microelectrode was surgically fixed in the caudate-putamen area of the brain in the rats, where fast-scan cyclic voltammetry (FSCV) was employed to detect DA and measure concentration of about 1 μM with the duration of 4 s [130]. These sensing strategies represent the possibility of a compact, wearable, wireless, battery-powered electrochemical device for the real-time monitoring of neurotransmitters with high sensitivity and low-power consumption. Another in vivo method for the detection of DA was designed under the consideration of the reduction of biofouling (Figure 9) [131]. The combination of photochemistry with electrochemical analysis provided a sensing strategy for the selective recognition of DA with a sensitivity of 0.15 nM. For this method, the author used DA as a sensitizer and target molecule, where the rationale behind the use of the photoelectrochemical method related to the prediction that it would provide a self-cleaning ability to the electrode [132]. In Figure 10, DA release was induced by ACh, which was injected into larval stage *Drosophila melanogaster* Canton S by pressure

injection. The current was measured with a carbon-fiber microelectrode using FSCV. The shape of the voltammogram confirmed the release of DA, while the brain was under the influence of ACh [133].

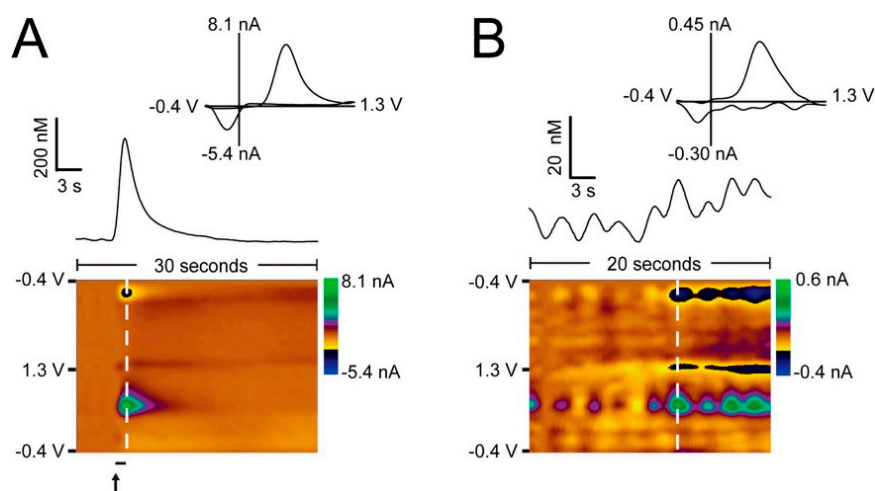


Figure 9. In vivo measurements of dopamine release using a PEDOT/Nafion-coated carbon-fiber microelectrode. Current versus time traces were extracted from the color plot at the peak oxidation potential for dopamine (~600 mV). The representative cyclic voltammograms were taken from the vertical white dashed line on the color plots. (A) Dopamine release was electrically evoked by stimulation (black bar, 40 pulses at 60 Hz, $\pm 150 \mu\text{A}$, 2 ms per phase) of the medial forebrain bundle and monitored in the nucleus accumbens of a Sprague-Dawley rat. (B) Spontaneous transients recorded in the nucleus accumbens of an isoflurane-anesthetized Sprague-Dawley rat [131]. Copyright 2015, American Chemical Society.

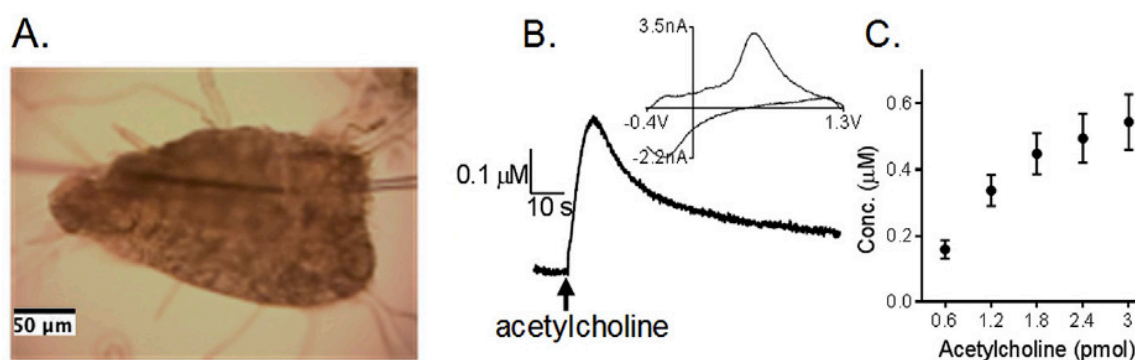


Figure 10. Acetylcholine-stimulated dopamine release in a *Drosophila melanogaster* ventral nerve cord (VNC). (A) Image showing electrode and stimulating pipet placed in VNC. (B) Acetylcholine (1.8 pmol) stimulated dopamine release measured with fast-scan cyclic voltammetry (FSCV). (C) Evoked dopamine concentration as a function of the amount of acetylcholine [133]. Copyright 2018, Elsevier.

As shown in Figure 11, the quantification of 5-HT was performed in an embryonic zebrafish intestine under physiological conditions with the implanted microelectrodes at different sites in the intestine, where the DPV showed a well-defined peak at 360 mV versus the Ag/AgCl electrode. The information obtained from this study has been used in the study of development mechanisms and the control of gastrointestinal functions [134]. Swamy and Venton reported on the development CNT-modified microelectrodes for the detection of 5-HT with reduced electrode biofouling from the oxidation byproducts of serotonin. In this work, the effect of nanotubes on the electron transfer kinetics, electrode response time, electrode fouling, and the in vivo detection of DA and 5-HT were

studied [135]. It was suggested that a larger electrode with nanotube coatings and slow electrochemical analysis might not be suitable for the *in vivo* analysis of neurotransmitters. FSCV and fast-scan controlled adsorption voltammetry (FSCAV) have been used to detect the presence of serotonin and its raised levels in the hippocampus of mice [136]. This study demonstrated the detection of an ambient extracellular serotonin level of 64.9 nM. The obtained electrochemical data was validated using a pharmacological approach, and interference by DA and NE were avoided. A poly (3,4-ethylenedioxythiophene)/CNT-modified acupuncture needle was used for the real-time detection of 5-HT in a rat [137]. Figure 12 shows the insertion of the electrode into the limb of an intraperitoneal anesthetized rat. During the addition of different concentrations of 5-HT through microinjection, the amperometric response was recorded at an applied constant potential of 0.5 V. The modified acupuncture needle served as sensing platform. This detection approach is like spiked sample analysis. Further research and development is required to monitor and detect the presence of ultralow concentrations of neurotransmitters.

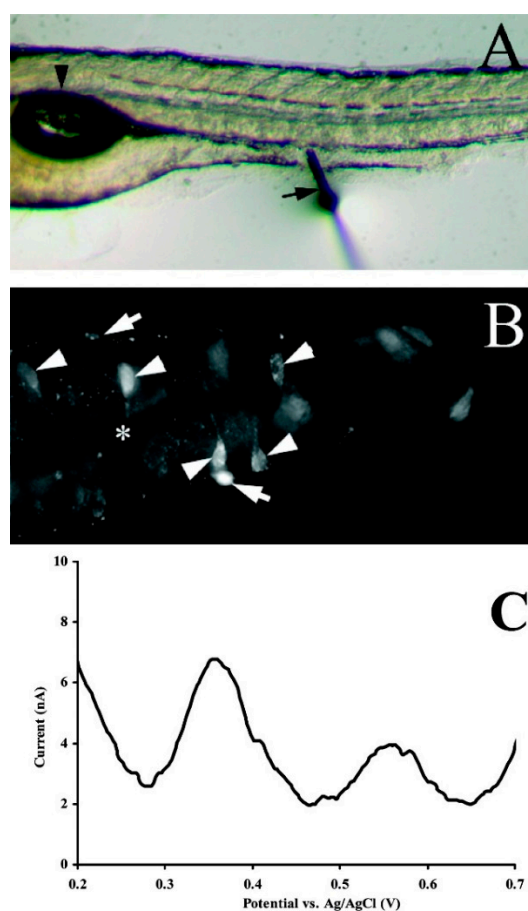


Figure 11. (A) Insertion of the electrochemical microsensor into the intact embryonic intestine between the posterior swim bladder and the end of the intestine at 5 dpf. The arrowhead indicates the swim bladder and the arrow shows the point of insertion of the microelectrodes. (B) 5-HT immunohistochemistry reveals a subset of enteric neurons (arrows), as well as enterochromaffin cells within the epithelium (arrowheads). Enteric neurons are on the periphery of the intestine between the thin circular and longitudinal smooth muscle layers. Enterochromaffin cells, which are situated more toward the basal surface of the epithelium, sense the contents of the lumen (asterisk) using thin processes. (C) Typical differential pulse voltammogram obtained *in vivo* with the implanted microelectrode as shown in (A). The supporting electrolyte was E3 medium [134]. Copyright 2010, American Chemical Society.

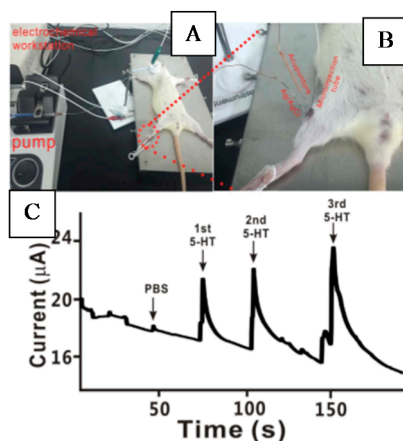


Figure 12. In vivo monitoring of 5-HT. (A) a photograph of the real-time and in vivo experiment after the rat was intraperitoneally anesthetized; (B) A zoomed picture; (C) the real-time recording of the inserted PEDOT/CNT/acupuncture needle in ST 36 upon the repeated injection of 10 μL , 10^{-5} M of 5-HT. Operating potential, 0.5 V vs. Ag/AgCl [137]. Copyright 2016, Nature.

L-Glu was detected using a Pt microelectrode with an enzyme (GluOx) and Nafion-incorporated coating where potassium chloride (70 mM and 120 mM) induced release of L-Glu was studied in the striatum and frontal cortex of the anesthetized rat [138]. The signal durations for low levels of KCl at the frontal cortex were lower, whereas, for high concentrations, there was an increase in the signal duration. The in vivo detection of L-Glu and ascorbate was carried out simultaneously in the striatum of the rats using microsensors [139]. Following the detection of L-Glu after a few minutes, the current response was decreased due to the uptake of L-Glu from the extracellular space. The above statement was well analyzed by the addition of glutamate oxidase, which assists brain cells with the consumption of L-Glu. In such cases, the neurotransmitter may have been consumed and created deficiencies in localized regimes of the living organism. The in vivo measurements of Glu in the striatum and prefrontal cortex of freely moving mice proceeded using a ceramic-based enzyme-coated Pt microelectrode. A microelectrode array (MEA) was surgically fixed to the central nervous system (CNS) of live rodents 50–100 μm below the surface of the brain. The baseline correction was done, and the electrode was employed to analyze the injected L-Glu and its effects at 3, 5, and 7 days post-implantation [140]. The enzymatic MEA exhibited fast temporal resolution (less than 1 s), excellent spatial resolution (micron-scale), and low detection limits (≤ 200 nM). The dendrimer-attached Pt/MWCNTs demonstrated selective detection of L-Glu [141]. In the L-Glu analysis, aside from mutual interference of other neurochemicals, peroxide formation was the most problematic issue that affected the selectivity in the L-Glu biosensors [142].

A Pt/Ir wire was used to detect NO in tumor-bearing mice to predict the tumor characteristics [143]. Intratumorally, CV and chronoamperometry were measured for various injected volumes of NO, which initially exhibited an increase in peak intensity, followed by a gradually decrease. This is due to the measurement of exogenous NO and its consumption by the tumoral tissue. Hemin/MWCNT/CFMEs were engineered as a biomimetic sensor to investigate the measurement of NO in the brain. The developed microsensor exhibited an average sensitivity of $1.72 \text{ nA } \mu\text{M}^{-1}$ with a LOD of 25 nM [144]. These microsensors allowed the detection of exogenous NO and did not show any response for AA, DA, and nitrite. This may be due to the low concentration of interference molecules. In another study, the distribution, release, and modulation of NO in zebrafish embryo intestines were quantified using CFMEs. The distribution of NO was monitored by DPV at different sites of the zebrafish, demarcated as (1) anterior, (2) middle, and (3) posterior, where a high level of NO was detected in the middle segment ($3.78 \pm 0.64 \mu\text{M}$) in comparison with the anterior ($1.08 \pm 0.41 \mu\text{M}$) and posterior ($1.00 \pm 0.41 \mu\text{M}$). This study revealed the feasibility of the NO detection in the embryos [145].

Thus, *in vivo* measurements have been demonstrated for a number of neurotransmitters using various nanomaterials, showing that (i) monitoring of chemical changes within living tissue can be achieved; (ii) this may be useful for the diagnosis of diseases; and (iii) there is potential for control and manipulation of chemical changes within living tissue. The effective *in vivo* analysis of neurotransmitters will have significant applications, not only for medical diagnostics and therapeutics, but also for the investigation of the specific effects of drug molecules in animal models.

4. Summary and Outlook

The clinical sensing of neurotransmitters and nervous system-related biomolecules offers a greater understanding of the chemical reactions that occur in the brain, which might be employed as a diagnostic tool for myriad of brain diseases. The combination of nanotechnology and electrochemical analysis establishes an excellent model for the quantitative analysis of neurotransmitters under both *in vitro* and *in vivo* conditions. Due to the large surface area-to-volume ratio of the nanomaterials involved, higher populations of molecules may be entrapped, which may directly contribute to the more sensitive detection of neurotransmitters. There have been a number of nanomaterials developed, which have been proven to possess good sensitivity and enhanced stability for *in vitro* detection. However, their selectivity should be improved for real-time analysis or in animal models due to biofouling and interferent molecules. In these cases, the use of membrane-based sensors or combinations of micro dialysis might be involved. Over the last two decades, substantial efforts have been invested toward *in vivo* electrochemistry. Particularly, advances in nanoscience and technology have contributed significantly to the development of real-time sensors. Today, electrochemical techniques are widely used in the fabrication of nanomaterials, as well as for sensing purposes, due to their fast response, cost effectiveness, and spatially resolved neurochemical measurements in different biological systems. Although current technologies are suitable for *in vitro* analysis, further development of electrochemical sensors are critical for the *in vivo* monitoring of neurotransmitters in order to better understand the nervous system. Ongoing research in the design of advanced nanomaterials-based *in vivo* electrochemical sensors with high selectivity, sensitivity, and durability may present exciting new avenues in neuroscience. The understanding of the brain, CNS, and peripheral nervous system would provide unprecedented insights into the neurochemical basis of behavior and disease.

Funding: This research was funded by a Discovery Grant from the Natural Sciences and Engineering Research Council of Canada [NSERC RGPIN-2015-06248].

Acknowledgments: A.C. acknowledges NSERC and the Canada Foundation for Innovation (CFI) for the Canada Research Chair Award in Electrochemistry and Nanoscience.

Conflicts of Interest: The authors declare no conflicts of interest.

References

1. Chiara, G.D. The principles of nerve cell communication. *Alcohol Health Res. World* **1997**, *21*, 106–108.
2. Pearson, R.A. Neurotransmitters and neurotrophins. In *Retinal Development*; Sernagor, E., Eglen, S., Harris, B., Wong, R., Eds.; Cambridge University Press: Cambridge, UK, 2015; pp. 99–125. ISBN 9780511541629.
3. Soleymani, J. Advanced materials for optical sensing and biosensing of neurotransmitters. *Trends Anal. Chem.* **2015**, *72*, 27–44. [[CrossRef](#)]
4. Si, B.; Song, E. Recent advances in the detection of neurotransmitters. *Chemosensors* **2018**, *6*, 1. [[CrossRef](#)]
5. Perry, M.; Li, Q.; Kennedy, R.T. Review of recent advances in analytical techniques for the determination of neurotransmitters. *Anal. Chim. Acta* **2009**, *653*, 1–22. [[CrossRef](#)] [[PubMed](#)]
6. Grieshaber, D.; MacKenzie, R.; Vörös, J.; Reimhult, E. Electrochemical biosensors—Sensor principles and architectures. *Sensors* **2008**, *8*, 1400–1458. [[CrossRef](#)] [[PubMed](#)]
7. Kimmel, D.W.; Leblanc, G.; Meschievitz, M.E.; Cliffel, D.E. Electrochemical sensors and biosensors. *Anal. Chem.* **2012**, *84*, 685–707. [[CrossRef](#)] [[PubMed](#)]

8. Chen, A.; Shah, B. Electrochemical sensing and biosensing based on square wave voltammetry. *Anal. Methods* **2013**, *5*, 2158–2173. [[CrossRef](#)]
9. Sáenz, H.S.C.; Hernández-Saravia, L.P.; Selva, J.S.G.; Sukeri, A.; Espinoza-Montero, P.J.; Bertotti, M. Electrochemical dopamine sensor using a nanoporous gold microelectrode: A proof-of-concept study for the detection of dopamine release by scanning electrochemical microscopy. *Microchim. Acta* **2018**, *185*, 1–9. [[CrossRef](#)] [[PubMed](#)]
10. Luo, X.; Morrin, A.; Killard, A.J.; Smyth, M.R. Application of nanoparticles in electrochemical sensors and biosensors. *Electroanalysis* **2006**, *18*, 319–326. [[CrossRef](#)]
11. Farka, Z.; Juřík, T.; Kovář, D.; Trnková, L.; Skládal, P. Nanoparticle-based immunochemical biosensors and assays: Recent advances and challenges. *Chem. Rev.* **2017**, *117*, 9973–10042. [[CrossRef](#)] [[PubMed](#)]
12. Nakajima, A. Application of single-electron transistor to biomolecule and ion sensors. *Appl. Sci.* **2016**, *6*, 94. [[CrossRef](#)]
13. Turkevich, J.; Cooper Stevenson, P. A study of the nucleation and growth processes in the synthesis of colloidal gold. *Discuss. Faraday Soc.* **1951**, *11*, 55–75. [[CrossRef](#)]
14. Murphy, C.J.; Gole, A.M.; Stone, J.W.; Sisco, P.N.; Alkilany, A.M.; Goldsmith, E.C.; Baxter, S.C. Gold nanoparticles in biology: Beyond toxicity to cellular imaging. *Acc. Chem. Res.* **2008**, *41*, 1721–1730. [[CrossRef](#)] [[PubMed](#)]
15. Xiao, Y. “Plugging into enzymes”: Nanowiring of redox enzymes by a gold nanoparticle. *Science* **2003**, *299*, 1877–1881. [[CrossRef](#)] [[PubMed](#)]
16. Zhuo, Y.; Yuan, R.; Chai, Y.; Tang, D.; Zhang, Y.; Wang, N.; Li, X.; Zhu, Q. A reagentless amperometric immunosensor based on gold nanoparticles/thionine/Nafion-membrane-modified gold electrode for determination of α -1-fetoprotein. *Electrochem. Commun.* **2005**, *7*, 355–360. [[CrossRef](#)]
17. Pan, M.; Gu, Y.; Yun, Y.; Li, M.; Jin, X.; Wang, S. Nanomaterials for electrochemical immunosensing. *Sensors* **2017**, *17*, 1041. [[CrossRef](#)]
18. Rajakumar, G.; Gomathi, T.; Rahuman, A.A.; Thiruvengadam, M.; Mydhili, G.; Kim, S.; Lee, T. Biosynthesis and biomedical applications of gold nanoparticles using *Eclipta prostrata* leaf extract. *Appl. Sci.* **2016**, *6*, 222. [[CrossRef](#)]
19. Li, H.; Sun, Z.; Zhong, W.; Hao, N.; Xu, D.; Chen, H. Arrays based on silver nanoparticle aggregates. *Anal. Chem.* **2010**, *82*, 5477–5483. [[CrossRef](#)] [[PubMed](#)]
20. Oliveira, O.N.; Iost, R.M.; Siqueira, J.R.; Crespilho, F.N.; Caseli, L. Nanomaterials for Diagnosis: Challenges and applications in smart devices based on molecular recognition. *ACS Appl. Mater. Interfaces* **2014**, *6*, 14745–14766. [[CrossRef](#)] [[PubMed](#)]
21. Xia, Y.; Xiong, Y.; Lim, B.; Skrabalak, S.E. Shape-controlled synthesis of metal nanocrystals: Simple chemistry meets complex physics? *Angew. Chem.* **2009**, *48*, 60–103. [[CrossRef](#)] [[PubMed](#)]
22. Adhikari, B.R.; Govindhan, M.; Chen, A. Carbon nanomaterials based electrochemical sensors/biosensors for the sensitive detection of pharmaceutical and biological compounds. *Sensors* **2015**, *15*, 22490–22508. [[CrossRef](#)] [[PubMed](#)]
23. Chatterjee, S.; Chen, A. Nanomaterials based electrochemical sensors for biomedical applications. *Chem. Soc. Rev.* **2013**, *42*, 5425–5438. [[CrossRef](#)]
24. Iijima, S. Helical microtubules of graphitic carbon. *Nature* **1991**, *354*, 56–58. [[CrossRef](#)]
25. Wildöer, J.W.G.; Venema, L.C.; Rinzler, A.G.; Smalley, R.E.; Dekker, C. Electronic structure of atomically resolved carbon nanotubes. *Nature* **1998**, *391*, 59–62. [[CrossRef](#)]
26. Govindhan, M.; Liu, Z.; Chen, A. Design and electrochemical study of platinum-based nanomaterials for sensitive detection of nitric oxide in biomedical applications. *Nanomaterials* **2016**, *6*, 211. [[CrossRef](#)] [[PubMed](#)]
27. Maduraiveeran, G.; Sasidharan, M.; Ganesan, V. Electrochemical sensor and biosensor platforms based on advanced nanomaterials for biological and biomedical applications. *Biosens. Bioelectron.* **2018**, *103*, 113–129. [[CrossRef](#)] [[PubMed](#)]
28. Chatterjee, S.; Wen, J.; Chen, A. Electrochemical determination of methylglyoxal as a biomarker in human plasma. *Biosens. Bioelectron.* **2013**, *42*, 349–354. [[CrossRef](#)] [[PubMed](#)]
29. McAllister, M.J.; Li, J.; Adamson, D.H.; Schniepp, H.C.; Abdala, A.A.; Liu, J.; Herrera-Alonso, M.; Milius, D.L.; Car, R.; Prud'homme, R.K.; et al. A single sheet functionalized graphene by oxidation and thermal expansion of graphite. *Chem. Mater.* **2007**, *19*, 4396–4404. [[CrossRef](#)]

30. Sidhureddy, B.; Thiruppathi, A.R.; Chen, A. From graphite to interconnected reduced graphene oxide: One-pot synthesis and supercapacitor application. *Chem. Commun.* **2017**, *53*, 7828–7831. [[CrossRef](#)] [[PubMed](#)]
31. Wang, Z.; Ciacchi, L.C.; Wei, G. Recent advances in the synthesis of graphene-based nanomaterials for controlled drug delivery. *Appl. Sci.* **2017**, *7*, 1175. [[CrossRef](#)]
32. Tian, W.; Liu, X.; Yu, W. Research progress of gas sensor based on graphene and its derivatives: A Review. *Appl. Sci.* **2018**, *8*, 1118. [[CrossRef](#)]
33. Garnayak, S.; Patel, S. Oxidation of epinephrine to adrenochrome by cetyltrimethylammonium dichromate: A mechanistic study. *Ind. Eng. Chem. Res.* **2014**, *53*, 12249–12256. [[CrossRef](#)]
34. van der Valk, J.P.M.; Berends, I.; Gerth van Wijk, R.; Arends, N.J.T.; van Maaren, M.S.; de Groot, H.; Wichers, H.J.; Emons, J.A.M.; Dubois, A.E.J.; de Jong, N.W. Small percentage of anaphylactic reactions treated with epinephrine during food challenges in Dutch children. *Ann. Allergy Asthma Immunol.* **2017**, *120*, 300–303. [[CrossRef](#)] [[PubMed](#)]
35. Dong, W.; Ren, Y.; Bai, Z.; Jiao, J.; Chen, Y.; Han, B.; Chen, Q. Synthesis of tetrahedral Au-Pd core-shell nanocrystals and reduction of graphene oxide for the electrochemical detection of epinephrine. *J. Colloid Interface Sci.* **2018**, *512*, 812–818. [[CrossRef](#)] [[PubMed](#)]
36. Wierzbicka, E.; Sulka, G.D. Nanoporous spongelike Au-Ag films for electrochemical epinephrine sensing. *J. Electroanal. Chem.* **2016**, *762*, 43–50. [[CrossRef](#)]
37. Wierzbicka, E.; Sulka, G.D. Fabrication of highly ordered nanoporous thin Au films and their application for electrochemical determination of epinephrine. *Sens. Actuators B Chem.* **2016**, *222*, 270–279. [[CrossRef](#)]
38. Beitollahi, H.; Karimi-Maleh, H.; Khabazzadeh, H. Nanomolar and selective determination of epinephrine in the presence of norepinephrine using carbon paste electrode modified with carbon nanotubes and novel 2-(4-oxo-3-phenyl-3,4-dihydro-quinazolinyl)-N'-phenyl-hydrazinecarbothioamide. *Anal. Chem.* **2008**, *80*, 9848–9851. [[CrossRef](#)] [[PubMed](#)]
39. Li, H.-H.; Wang, H.-H.; Li, W.-T.; Fang, X.-X.; Guo, X.-C.; Zhou, W.-H.; Cao, X.; Kou, D.-X.; Zhou, Z.-J.; Wu, S.-X. A novel electrochemical sensor for epinephrine based on three dimensional molecularly imprinted polymer arrays. *Sens. Actuators B Chem.* **2016**, *222*, 1127–1133. [[CrossRef](#)]
40. Urdaneta, I.; Keller, A.; Atabek, O.; Palma, J.L.; Finkelstein-Shapiro, D.; Tarakeshwar, P.; Mujica, V.; Calatayud, M. Dopamine adsorption on TiO₂ anatase surfaces. *J. Phys. Chem. C* **2014**, *118*, 20688–20693. [[CrossRef](#)]
41. Larkin, B.A.J.; El-Sayed, M.; Brownson, D.A.C.; Banks, C.E. Crime scene investigation III: Exploring the effects of drugs of abuse and neurotransmitters on bloodstain pattern analysis. *Anal. Methods* **2012**, *4*, 721–729. [[CrossRef](#)]
42. Khan, A.F.; Brownson, D.A.C.; Randviir, E.P.; Smith, G.C.; Banks, C.E. 2D hexagonal boron nitride (2D-hBN) explored for the electrochemical sensing of dopamine. *Anal. Chem.* **2016**, *88*, 9729–9737. [[CrossRef](#)] [[PubMed](#)]
43. Peeters, M.M.; van Grinsven, B.; Foster, C.W.; Cleij, T.J.; Banks, C.E. Introducing thermal wave transport analysis (TWTA): A thermal technique for dopamine detection by screen-printed electrodes functionalized with molecularly imprinted polymer (MIP) particles. *Molecules* **2016**, *21*, 552. [[CrossRef](#)] [[PubMed](#)]
44. Stout, K.A.; Dunn, A.R.; Lohr, K.M.; Alter, S.P.; Cliburn, R.A.; Guillot, T.S.; Miller, G.W. Selective enhancement of dopamine release in the ventral pallidum of methamphetamine-sensitized mice. *ACS Chem. Neurosci.* **2016**, *7*, 1364–1373. [[CrossRef](#)] [[PubMed](#)]
45. Savitt, J.; Dawson, V.; Dawson, T. Diagnosis and treatment of Parkinson disease: Molecules to medicine. *J. Clin. Investig.* **2006**, *116*, 1744–1754. [[CrossRef](#)] [[PubMed](#)]
46. Song, W.; Chen, Y.; Xu, J.; Yang, X.; Tian, D.-B. Dopamine sensor based on molecularly imprinted electrosynthesized polymers. *J. Solid State Electrochem.* **2010**, *14*, 1909–1914. [[CrossRef](#)]
47. Lacher, N.A.; Lunte, S.M.; Martin, R.S. Development of a microfabricated palladium decoupler/electrochemical detector for microchip capillary electrophoresis using a hybrid glass/poly(dimethylsiloxane) device. *Anal. Chem.* **2004**, *76*, 2482–2491. [[CrossRef](#)] [[PubMed](#)]
48. Tyagi, P.; Postetter, D.; Saragnese, D.L.; Randall, C.L.; Mirski, M.A.; Gracias, D.H. Patternable nanowire sensors for electrochemical recording of dopamine. *Anal. Chem.* **2009**, *81*, 9979–9984. [[CrossRef](#)] [[PubMed](#)]
49. Fabregat, G.; Estrany, F.; Casas, M.T.; Alemán, C.; Armelin, E. Detection of dopamine using chemically synthesized multilayered hollow microspheres. *J. Phys. Chem. B* **2014**, *118*, 4702–4709. [[CrossRef](#)] [[PubMed](#)]

50. Liao, C.; Zhang, M.; Niu, L.; Zheng, Z.; Yan, F. Organic electrochemical transistors with graphene-modified gate electrodes for highly sensitive and selective dopamine sensors. *J. Mater. Chem. B* **2014**, *2*, 191–200. [[CrossRef](#)]
51. Teymourian, H.; Salimi, A.; Khezrian, S. Fe₃O₄ magnetic nanoparticles/reduced graphene oxide nanosheets as a novel electrochemical and bioelectrochemical sensing platform. *Biosens. Bioelectron.* **2013**, *49*, 1–8. [[CrossRef](#)] [[PubMed](#)]
52. Demuru, S.; Nela, L.; Marchack, N.; Holmes, S.J.; Farmer, D.B.; Tulevski, G.S.; Lin, Q.; Deligianni, H. Scalable Nanostructured Carbon Electrode Arrays for Enhanced Dopamine Detection. *ACS Sens.* **2018**, *3*, 799–805. [[CrossRef](#)] [[PubMed](#)]
53. Ma, X.; Chao, M.; Wang, Z. Electrochemical detection of dopamine in the presence of epinephrine, uric acid and ascorbic acid using a graphene-modified electrode. *Anal. Methods* **2012**, *4*, 1687–1692. [[CrossRef](#)]
54. Oleinick, A.; Zhu, F.; Yan, J.; Mao, B.; Svir, I.; Amatore, C. Theoretical investigation of generator-collector microwell arrays for improving electroanalytical selectivity: Application to selective dopamine detection in the presence of ascorbic acid. *ChemPhysChem* **2013**, *14*, 1887–1898. [[CrossRef](#)] [[PubMed](#)]
55. Kannan, P.K.; Moshkalev, S.A.; Rout, C.S. Highly sensitive and selective electrochemical dopamine sensing properties of multilayer graphene nanobelts. *Nanotechnology* **2016**, *27*, 075504. [[CrossRef](#)] [[PubMed](#)]
56. Figueiredo-filho, L.C.S.; Silva, T.A.; Vicentini, F.C.; Fatibello-filho, O. Simultaneous voltammetric determination of dopamine and epinephrine in human body fluid samples using a glassy carbon electrode modified with nickel oxide nanoparticles and carbon nanotubes within a dihexadecylphosphate film. *Analyst* **2014**, *139*, 2842–2849. [[CrossRef](#)] [[PubMed](#)]
57. Oh, J.; Lee, J.S.; Jun, J.; Kim, S.G.; Jang, J. Ultrasensitive and Selective Organic FET-type Nonenzymatic Dopamine Sensor Based on Platinum Nanoparticles-Decorated Reduced Graphene Oxide. *ACS Appl. Mater. Interfaces* **2017**, *9*, 39526–39533. [[CrossRef](#)] [[PubMed](#)]
58. Álvarez-Martos, I.; Ferapontova, E.E. Electrochemical label-free aptasensor for specific analysis of dopamine in serum in the presence of structurally related neurotransmitters. *Anal. Chem.* **2016**, *88*, 3608–3616. [[CrossRef](#)] [[PubMed](#)]
59. Demuru, S.; Deligianni, H. Surface PEDOT:Nafion coatings for enhanced dopamine, serotonin and adenosine sensing. *J. Electrochem. Soc.* **2017**, *164*, G129–G138. [[CrossRef](#)]
60. Sharma, S.; Singh, N.; Tomar, V.; Chandra, R. A review on electrochemical detection of serotonin based on surface modified electrodes. *Biosens. Bioelectron.* **2018**, *106*, 76–93. [[CrossRef](#)] [[PubMed](#)]
61. Cesarino, I.; Galesco, H.V.; Machado, S.A.S. Determination of serotonin on platinum electrode modified with carbon nanotubes/polypyrrole/silver nanoparticles nanohybrid. *Mater. Sci. Eng. C* **2014**, *40*, 49–54. [[CrossRef](#)] [[PubMed](#)]
62. Tertiş, M.; Cernat, A.; Lacatiş, D.; Florea, A.; Bogdan, D.; Suci, M.; Săndulescu, R.; Cristea, C. Highly selective electrochemical detection of serotonin on polypyrrole and gold nanoparticles-based 3D architecture. *Electrochem. Commun.* **2017**, *75*, 43–47. [[CrossRef](#)]
63. Ran, G.; Chen, X.; Xia, Y. Electrochemical detection of serotonin based on a poly(bromocresol green) film and Fe₃O₄ nanoparticles in a chitosan matrix. *RSC Adv.* **2017**, *7*, 1847–1851. [[CrossRef](#)]
64. Zestos, A.G.; Jacobs, C.B.; Trikantopoulos, E.; Ross, A.E.; Venton, B.J. Polyethylenimine carbon nanotube fiber electrodes for enhanced detection of neurotransmitters. *Anal. Chem.* **2014**, *86*, 8568–8575. [[CrossRef](#)] [[PubMed](#)]
65. Ostock, C.Y.; Bhide, N.; Goldenberg, A.A.; George, J.A.; Bishop, C. Striatal norepinephrine efflux in L-DOPA-induced dyskinesia. *Neurochem. Int.* **2018**, *114*, 85–98. [[CrossRef](#)] [[PubMed](#)]
66. Townsend, A.D.; Wilken, G.H.; Mitchell, K.K.; Martin, R.S.; Macarthur, H. Simultaneous analysis of vascular norepinephrine and ATP release using an integrated microfluidic system. *J. Neurosci. Methods* **2016**, *266*, 68–77. [[CrossRef](#)] [[PubMed](#)]
67. Hamzaoui, O.; Jozwiak, M.; Geffriaud, T.; Sztrymf, B.; Prat, D.; Jacobs, F.; Monnet, X.; Trouiller, P.; Richard, C.; Teboul, J.L. Norepinephrine exerts an inotropic effect during the early phase of human septic shock. *Br. J. Anaesth.* **2018**, *120*, 517–524. [[CrossRef](#)] [[PubMed](#)]
68. Law, Y.M.; Plonka, C.M.; Feingold, B. Norepinephrine levels in children with single ventricle circulation. *Prog. Pediatr. Cardiol.* **2017**, *47*, 58–63. [[CrossRef](#)]
69. Samdani, K.J.; Joh, D.W.; Rath, M.K.; Lee, K.T. Electrochemical mediatorless detection of norepinephrine based on MoO₃ nanowires. *Electrochim. Acta* **2017**, *252*, 268–274. [[CrossRef](#)]

70. Samdani, K.J.; Samdani, J.S.; Kim, N.H.; Lee, J.H. FeMoO₄ based, enzyme-free electrochemical biosensor for ultrasensitive detection of norepinephrine. *Biosens. Bioelectron.* **2016**, *81*, 445–453. [[CrossRef](#)] [[PubMed](#)]
71. Beitollahi, H.; Mohammadi, S. Selective voltammetric determination of norepinephrine in the presence of acetaminophen and tryptophan on the surface of a modified carbon nanotube paste electrode. *Mater. Sci. Eng. C* **2013**, *33*, 3214–3219. [[CrossRef](#)] [[PubMed](#)]
72. Vilian, A.T.E.; Chen, S.M.; Hung, Y.T.; Ali, M.A.; Al-Hemaid, F.M.A. Electrochemical oxidation and determination of norepinephrine in the presence of acetaminophen using MnO₂ nanoparticle decorated reduced graphene oxide sheets. *Anal. Methods* **2014**, *6*, 6504–6513. [[CrossRef](#)]
73. Dai, M.; Haselwood, B.; Vogt, B.D.; La Belle, J.T. Amperometric sensing of norepinephrine at picomolar concentrations using screen printed, high surface area mesoporous carbon. *Anal. Chim. Acta* **2013**, *788*, 32–38. [[CrossRef](#)] [[PubMed](#)]
74. Atta, N.F.; Galal, A.; Azab, S.M. Electrochemical determination of neurotransmitters using gold nanoparticles on nafion/carbon paste modified electrode. *J. Electrochem. Soc.* **2012**, *159*, H765–H771. [[CrossRef](#)]
75. Atta, N.F.; Ali, S.M.; El-Ads, E.H.; Galal, A. The electrochemistry and determination of some neurotransmitters at SrPdO₃ modified graphite electrode. *J. Electrochem. Soc.* **2013**, *160*, G3144–G3151. [[CrossRef](#)]
76. Suárez-Pozos, E.; Martínez-Lozada, Z.; Méndez-Flores, O.G.; Guillem, A.M.; Hernández-Kelly, L.C.; Castelán, F.; Olivares-Bañuelos, T.N.; Chi-Castañeda, D.; Najimi, M.; Ortega, A. Characterization of the cystine/glutamate antiporter in cultured Bergmann glia cells. *Neurochem. Int.* **2017**, *106*, 52–59. [[CrossRef](#)] [[PubMed](#)]
77. Yu, L.J.; Wall, B.A.; Wangari-Talbot, J.; Chen, S. Metabotropic glutamate receptors in cancer. *Neuropharmacology* **2017**, *115*, 193–202. [[CrossRef](#)] [[PubMed](#)]
78. Bai, W.; Li, P.; Ning, Y.-L.; Peng, Y.; Xiong, R.-P.; Yang, N.; Chen, X.; Zhou, Y.-G. Adenosine A_{2A} receptor inhibition restores the normal transport of endothelial glutamate transporters in the brain. *Biochem. Biophys. Res. Commun.* **2018**, *498*, 795–802. [[CrossRef](#)] [[PubMed](#)]
79. Sirca, D.; Vardeu, A.; Pinna, M.; Diana, M.; Enrico, P. A robust, state-of-the-art amperometric microbiosensor for glutamate detection. *Biosens. Bioelectron.* **2014**, *61*, 526–531. [[CrossRef](#)] [[PubMed](#)]
80. Burmeister, J.J.; Gerhardt, G.A. Self-referencing ceramic-based multisite microelectrodes for the detection and elimination of interferences from the measurement of L-glutamate and other analytes. *Anal. Chem.* **2001**, *73*, 1037–1042. [[CrossRef](#)] [[PubMed](#)]
81. Huang, X.J.; Im, H.S.; Lee, D.H.; Kim, H.S.; Choi, Y.K. Ferrocene functionalized single-walled carbon nanotube bundles. Hybrid interdigitated construction film for L-glutamate detection. *J. Phys. Chem. C* **2007**, *106*, 1200–1206. [[CrossRef](#)]
82. Dorozhko, E.V.; Korotkova, E.I.; Shabaeva, A.A.; Mosolkov, A.Y. Electrochemical determination of L-glutamate on a carbon-containing electrode modified with gold by voltammetry. *Procedia Chem.* **2015**, *15*, 365–370. [[CrossRef](#)]
83. Batra, B.; Pundir, C.S. An amperometric glutamate biosensor based on immobilization of glutamate oxidase onto carboxylated multiwalled carbon nanotubes/gold nanoparticles/chitosan composite film modified Au electrode. *Biosens. Bioelectron.* **2013**, *47*, 496–501. [[CrossRef](#)] [[PubMed](#)]
84. Freudenberg, F.; Altho, A.; Reif, A. Neuronal nitric oxide synthase (NOS1) and its adaptor, NOS1AP, as a genetic risk factors for psychiatric disorders. *Genes Brain Behav.* **2015**, *14*, 46–63. [[CrossRef](#)] [[PubMed](#)]
85. Kiss, J.P.; Vizi, E.S. Nitric oxide: A novel link between synaptic and nonsynaptic transmission. *Trends Neurosci.* **2001**, *24*, 211–215. [[CrossRef](#)]
86. Balamurugan, M.; Madasamy, T.; Pandiaraj, M.; Bhargava, K.; Sethy, N.K.; Karunakaran, C. Electrochemical assay for the determination of nitric oxide metabolites using copper(II) chlorophyllin modified screen printed electrodes. *Anal. Biochem.* **2015**, *478*, 121–127. [[CrossRef](#)] [[PubMed](#)]
87. Govindhan, M.; Chen, A. Enhanced electrochemical sensing of nitric oxide using a nanocomposite consisting of platinum-tungsten nanoparticles, reduced graphene oxide and an ionic liquid. *Microchim. Acta* **2016**, *183*, 2879–2887. [[CrossRef](#)]
88. Liu, Z.; Forsyth, H.; Khaper, N.; Chen, A. Sensitive electrochemical detection of nitric oxide based on AuPt and reduced graphene oxide nanocomposites. *Analyst* **2016**, *141*, 4074–4083. [[CrossRef](#)] [[PubMed](#)]

89. Liu, Z.; Nemeč-Bakk, A.; Khaper, N.; Chen, A. Sensitive electrochemical detection of nitric oxide release from cardiac and cancer cells via a hierarchical nanoporous gold microelectrode. *Anal. Chem.* **2017**, *89*, 8036–8043. [[CrossRef](#)] [[PubMed](#)]
90. König, M.; Thinnies, A.; Klein, J. Microdialysis and its use in behavioural studies: Focus on acetylcholine. *J. Neurosci. Methods* **2018**, *300*, 206–215. [[CrossRef](#)] [[PubMed](#)]
91. Perry, E.; Walker, M.; Grace, J.; Perry, R. Acetylcholine in mind: A neurotransmitter correlate of consciousness? *Trends Neurosci.* **1999**, *22*, 273–280. [[CrossRef](#)]
92. Akhtar, M.H.; Hussain, K.K.; Gurudatt, N.G.; Shim, Y.B. Detection of Ca²⁺-induced acetylcholine released from leukemic T-cells using an amperometric microfluidic sensor. *Biosens. Bioelectron.* **2017**, *98*, 364–370. [[CrossRef](#)] [[PubMed](#)]
93. Tian, Y.; Ye, S.; Shi, X.; Jing, L.; Liang, C.; Xian, Y. An electrochemical platform for acetylcholinesterase activity assay and inhibitors screening based on Michael addition reaction between thiocholine and catechol-terminated SAMs. *Analyst* **2011**, *136*, 5084–5090. [[CrossRef](#)] [[PubMed](#)]
94. Chauhan, N.; Pundir, C.S. Amperometric determination of acetylcholine—A neurotransmitter, by chitosan/gold-coated ferric oxide nanoparticles modified gold electrode. *Biosens. Bioelectron.* **2014**, *61*, 1–8. [[CrossRef](#)] [[PubMed](#)]
95. Bolat, E.Ö.; Tığ, G.A.; Pekyardımcı, Ş. Fabrication of an amperometric acetylcholine esterase-choline oxidase biosensor based on MWCNTs-Fe₃O₄ NPs-CS nanocomposite for determination of acetylcholine. *J. Electroanal. Chem.* **2017**, *785*, 241–248. [[CrossRef](#)]
96. Aynaci, E.; Yaşar, A.; Arslan, F. An amperometric biosensor for acetylcholine determination prepared from acetylcholinesterase-choline oxidase immobilized in polypyrrole-polyvinylsulfonate film. *Sens. Actuators B Chem.* **2014**, *202*, 1028–1036. [[CrossRef](#)]
97. Ralevic, V. Purines as neurotransmitters and neuromodulators in blood vessels. *Curr. Vasc. Pharmacol.* **2009**, *7*, 3–14. [[CrossRef](#)] [[PubMed](#)]
98. Zuo, X.; Song, S.; Zhang, J.; Pan, D.; Wang, L.; Fan, C. A target-responsive electrochemical aptamer switch (TREAS) for reagentless detection of nanomolar ATP. *J. Am. Chem. Soc.* **2007**, *129*, 1042–1043. [[CrossRef](#)] [[PubMed](#)]
99. Yu, J.; Zhang, L.; Xu, X.; Liu, S. Quantitative detection of potassium ions and adenosine triphosphate via a nanochannel-based electrochemical platform coupled with G-quadruplex aptamers. *Anal. Chem.* **2014**, *86*, 10641–10648. [[CrossRef](#)] [[PubMed](#)]
100. Wang, P.; Cheng, Z.; Chen, Q.; Qu, L.; Miao, X.; Feng, Q. Construction of a paper-based electrochemical biosensing platform for rapid and accurate detection of adenosine triphosphate (ATP). *Sens. Actuators B Chem.* **2018**, *256*, 931–937. [[CrossRef](#)]
101. Tsele, T.P.; Adekunle, A.S.; Fayemi, O.E.; Ebenso, E.E. Electrochemical detection of epinephrine using polyaniline nanocomposite films doped with TiO₂ and RuO₂ nanoparticles on multi-walled carbon nanotube. *Electrochim. Acta* **2017**, *243*, 331–348. [[CrossRef](#)]
102. Mao, H.; Zhang, H.; Jiang, W.; Liang, J.; Sun, Y.; Zhang, Y.; Wu, Q.; Zhang, G.; Song, X.M. Poly(ionic liquid) functionalized polypyrrole nanotubes supported gold nanoparticles: An efficient electrochemical sensor to detect epinephrine. *Mater. Sci. Eng. C* **2017**, *75*, 495–502. [[CrossRef](#)] [[PubMed](#)]
103. Ding, M.; Zhou, Y.; Liang, X.; Zou, H.; Wang, Z.; Wang, M.; Ma, J. An electrochemical sensor based on graphene / poly (brilliant cresyl blue) nanocomposite for determination of epinephrine. *J. Electroanal. Chem.* **2016**, *763*, 25–31. [[CrossRef](#)]
104. Mphuthi, N.G.; Adekunle, A.S.; Ebenso, E.E. Electrocatalytic oxidation of epinephrine and norepinephrine at metal oxide doped phthalocyanine/MWCNT composite sensor. *Sci. Rep.* **2016**, *6*, 26938. [[CrossRef](#)] [[PubMed](#)]
105. Chandrashekar, B.N.; Kumara Swamy, B.E.; Gururaj, K.J.; Cheng, C. Simultaneous determination of epinephrine, ascorbic acid and folic acid using TX-100 modified carbon paste electrode: A cyclic voltammetric study. *J. Mol. Liq.* **2017**, *231*, 379–385. [[CrossRef](#)]
106. Huang, Q.; Hu, S.; Zhang, H.; Chen, J.; He, Y.; Li, F.; Weng, W.; Ni, J.; Bao, X.; Lin, Y. Carbon dots and chitosan composite film based biosensor for the sensitive and selective determination of dopamine. *Analyst* **2013**, *138*, 5417–5423. [[CrossRef](#)] [[PubMed](#)]

107. Gao, G.; Zhang, Z.; Wang, K.; Yuan, Q.; Wang, X. One-pot synthesis of dendritic Pt₃Ni nanoalloys as nonenzymatic electrochemical biosensors with high sensitivity and selectivity for dopamine detection. *Nanoscale* **2017**, *9*, 10998–11003. [[CrossRef](#)] [[PubMed](#)]
108. Rand, E.; Periyakaruppan, A.; Tanaka, Z.; Zhang, D.; Marsh, M.P.; Andrews, R.J.; Lee, K.H.; Chen, B.; Meyyappan, M.; Koehne, J.E. A carbon nanofiber based biosensor for simultaneous detection of dopamine and serotonin in the presence of ascorbic acid. *Biosens. Bioelectron.* **2012**, *42*, 434–438. [[CrossRef](#)] [[PubMed](#)]
109. Anithaa, A.C.; Asokan, K.; Sekar, C. Highly sensitive and selective serotonin sensor based on gamma ray irradiated tungsten trioxide nanoparticles. *Sens. Actuators B Chem.* **2017**, *238*, 667–675. [[CrossRef](#)]
110. Wang, Y.; Wang, S.; Tao, L.; Min, Q.; Xiang, J.; Wang, Q.; Xie, J.; Yue, Y.; Wu, S.; Li, X.; et al. A disposable electrochemical sensor for simultaneous determination of norepinephrine and serotonin in rat cerebrospinal fluid based on MWNTs-ZnO/chitosan composites modified screen-printed electrode. *Biosens. Bioelectron.* **2015**, *65*, 31–38. [[CrossRef](#)] [[PubMed](#)]
111. Fayemi, O.E.; Adekunle, A.S.; Ebenso, E.E. Electrochemical determination of serotonin in urine samples based on metal oxide nanoparticles/MWCNT on modified glassy carbon electrode. *Sens. Bio-Sens. Res.* **2017**, *13*, 17–27. [[CrossRef](#)]
112. Lavanya, N.; Sekar, C. Electrochemical sensor for simultaneous determination of epinephrine and norepinephrine based on cetyltrimethylammonium bromide assisted SnO₂ nanoparticles. *J. Electroanal. Chem.* **2017**, *801*, 503–510. [[CrossRef](#)]
113. Chen, J.; Huang, H.; Zeng, Y.; Tang, H.; Li, L. A novel composite of molecularly imprinted polymer-coated PdNPs for electrochemical sensing norepinephrine. *Biosens. Bioelectron.* **2015**, *65*, 366–374. [[CrossRef](#)] [[PubMed](#)]
114. Dalkiran, B.; Erden, P.E.; Kilic, E. Graphene and tricobalt tetraoxide nanoparticles based biosensor for electrochemical glutamate sensing. *Artif. Cells Nanomed. Biotechnol.* **2017**, *45*, 340–348. [[CrossRef](#)] [[PubMed](#)]
115. Batra, B.; Kumari, S.; Pundir, C.S. Enzyme and microbial technology construction of glutamate biosensor based on covalent immobilization of glutamate oxidase on polypyrrole nanoparticles/polyaniline modified gold electrode. *Enzyme Microb. Technol.* **2014**, *57*, 69–77. [[CrossRef](#)] [[PubMed](#)]
116. Tolosa, V.M.; Wassum, K.M.; Maidment, N.T.; Monbouquette, H.G. Electrochemically deposited iridium oxide reference electrode integrated with an electroenzymatic glutamate sensor on a multi-electrode array microprobe. *Biosens. Bioelectron.* **2013**, *42*, 256–260. [[CrossRef](#)] [[PubMed](#)]
117. Yap, C.M.; Xu, G.Q.; Ang, S.G. Amperometric nitric oxide sensor based on nanoporous platinum phthalocyanine modified electrodes. *Anal. Chem.* **2013**, *85*, 106–113. [[CrossRef](#)] [[PubMed](#)]
118. Zhang, L.; Fang, Z.; Zhao, G.C.; Wei, X.W. Electrodeposited platinum nanoparticles on the multi-walled carbon nanotubes and its electrocatalytic for nitric oxide. *Int. J. Electrochem. Sci.* **2008**, *3*, 746–754.
119. Schuvailo, O.N.; Dzyadevych, S.V.; El'skaya, A.V.; Gauthier-Sauvigne, S.; Csoregi, E.; Cespeglio, R.; Soldatkin, A.P. Carbon fibre-based microbiosensors for in vivo measurements of acetylcholine and choline. *Biosens. Bioelectron.* **2005**, *21*, 87–94. [[CrossRef](#)] [[PubMed](#)]
120. Sattarahmady, N.; Heli, H.; Vais, R.D. An electrochemical acetylcholine sensor based on lichen-like nickel oxide nanostructure. *Biosens. Bioelectron.* **2013**, *48*, 197–202. [[CrossRef](#)] [[PubMed](#)]
121. Moreira, F.T.C.; Sale, M.G.F.; Di Lorenzo, M. Towards timely Alzheimer diagnosis: A self-powered amperometric biosensor for the neurotransmitter acetylcholine. *Biosens. Bioelectron.* **2017**, *87*, 607–614. [[CrossRef](#)] [[PubMed](#)]
122. Deng, C.; Xia, Y.; Xiao, C.; Nie, Z.; Yang, M.; Si, S. Electrochemical oxidation of purine and pyrimidines bases based on the boron-doped nanotube modified electrode. *Biosens. Bioelectron.* **2012**, *31*, 469–474. [[CrossRef](#)] [[PubMed](#)]
123. Shi, P.; Zhang, Y.; Yu, Z.; Zhang, S. Label-free electrochemical detection of ATP based on amino-functionalized metal-organic framework. *Sci. Rep.* **2017**, *7*, 6500. [[CrossRef](#)] [[PubMed](#)]
124. Ma, Y.; Zhao, H.; Yu, P.; Su, L.; Zhang, D.; Mao, L. Electrochemical sensing of ATP with synthetic cyclophane as recognition element. *Sci. China Ser. B Chem.* **2009**, *52*, 741–745. [[CrossRef](#)]
125. Sanghavi, B.J.; Sitaula, S.; Griep, M.H.; Karna, S.P.; Ali, M.F.; Swami, N.S. Real-time electrochemical monitoring of adenosine triphosphate in the picomolar to micromolar range using graphene-modified electrodes. *Anal. Chem.* **2013**, *85*, 8158–8165. [[CrossRef](#)] [[PubMed](#)]

126. Liang, Y.; Su, J.; Huang, Y.; Li, X.; Tao, Y.; Lu, C.; Zhu, J.; Bai, Z.; Meng, J.; Lu, X.; et al. An ATP aptasensor based on the peroxidase-like activity of hemin/graphene oxide nanosheets. *Anal. Sci.* **2016**, *32*, 565–569. [[CrossRef](#)] [[PubMed](#)]
127. Revilla, R.; Diez-Alarcia, R.; Mostany, R.; Perez, C.C.; Fernandez-Lopez, A. Norepinephrine, epinephrine and MHPG levels in chick brain development. *Neuropharmacology* **2001**, *41*, 480–485. [[CrossRef](#)]
128. Rees, H.R.; Anderson, S.E.; Privman, E.; Bau, H.H.; Venton, B.J. Carbon nanopipette electrodes for dopamine detection in *Drosophila*. *Anal. Chem.* **2015**, *87*, 3849–3855. [[CrossRef](#)] [[PubMed](#)]
129. Crespi, F. Wireless in vivo voltammetric measurements of neurotransmitters in freely behaving rats. *Biosens. Bioelectron.* **2010**, *25*, 2425–2430. [[CrossRef](#)] [[PubMed](#)]
130. Lin, N.S.; Wang, L.; Wang, M.X.; Xu, S.W.; Yu, W.D.; Cai, X.X. A wearable wireless electrochemical instrument used for *in-vivo* neurotransmitter detection. *Chin. J. Anal. Chem.* **2015**, *43*, 93–97. [[CrossRef](#)]
131. Vreeland, R.F.; Atcherley, C.W.; Russell, W.S.; Xie, J.Y.; Lu, D.; Laude, N.D.; Porreca, F.; Heien, M.L. Biocompatible PEDOT:Nafion composite electrode coatings for selective detection of neurotransmitters in vivo. *Anal. Chem.* **2015**, *87*, 2600–2607. [[CrossRef](#)] [[PubMed](#)]
132. Xin, Y.; Li, Z.; Wu, W.; Fu, B.; Wu, H.; Zhang, Z. Recognition unit-free and self-cleaning photoelectrochemical sensing platform on TiO₂ nanotube photonic crystals for sensitive and selective detection of dopamine release from mouse brain. *Biosens. Bioelectron.* **2017**, *87*, 396–403. [[CrossRef](#)] [[PubMed](#)]
133. Pyakurel, P.; Shin, M.; Venton, B.J. Nicotinic acetylcholine receptor (nAChR) mediated dopamine release in larval *Drosophila melanogaster*. *Neurochem. Int.* **2018**, *114*, 33–41. [[CrossRef](#)] [[PubMed](#)]
134. Njagi, J.; Ball, M.; Best, M.; Wallace, K.N.; Andreescu, S. Electrochemical quantification of serotonin in the live embryonic zebrafish intestine. *Anal. Chem.* **2010**, *82*, 1822–1830. [[CrossRef](#)] [[PubMed](#)]
135. Swamy, B.E.K.; Venton, B.J. Carbon nanotube-modified microelectrodes for simultaneous detection of dopamine and serotonin in vivo. *Analyst* **2007**, *132*, 876–884. [[CrossRef](#)] [[PubMed](#)]
136. Abdalla, A.; Atcherley, C.W.; Pathirathna, P.; Samaranyake, S.; Qiang, B.; Peña, E.; Morgan, S.L.; Heien, M.L.; Hashemi, P. In Vivo ambient serotonin measurements at carbon-fiber microelectrodes. *Anal. Chem.* **2017**, *89*, 9703–9711. [[CrossRef](#)] [[PubMed](#)]
137. Li, Y.-T.; Tang, L.-N.; Ning, Y.; Shu, Q.; Liang, F.-X.; Wang, H.; Zhang, G.-J. In vivo monitoring of serotonin by nanomaterial functionalized acupuncture needle. *Sci. Rep.* **2016**, *6*, 28018–28024. [[CrossRef](#)] [[PubMed](#)]
138. Day, B.K.; Pomerleau, F.; Burmeister, J.J.; Huettl, P.; Gerhardt, G.A. Microelectrode array studies of basal and potassium-evoked release of L-glutamate in the anesthetized rat brain. *J. Neurochem.* **2006**, *96*, 1626–1635. [[CrossRef](#)] [[PubMed](#)]
139. Kulagina, N.V.; Shankar, L.; Michael, A.C. Monitoring glutamate and ascorbate in the extracellular space of brain tissue with electrochemical microsensors. *Anal. Chem.* **1999**, *71*, 5093–5100. [[CrossRef](#)] [[PubMed](#)]
140. Hascup, E.R.; Hascup, K.N. Electrochemical techniques for subsecond neurotransmitter detection in live rodents. *Comp. Med.* **2014**, *64*, 249–255. [[PubMed](#)]
141. Yu, Y.; Sun, Q.; Zhou, T.; Zhu, M.; Jin, L.; Shi, G. On-line microdialysis system with poly(amidoamine)-encapsulated Pt nanoparticles biosensor for glutamate sensing in vivo. *Bioelectrochemistry* **2011**, *81*, 53–57. [[CrossRef](#)] [[PubMed](#)]
142. Wahono, N.; Qin, S.; Oomen, P.; Cremers, T.I.F.; de Vries, M.G.; Westerink, B.H.C. Evaluation of permselective membranes for optimization of intracerebral amperometric glutamate biosensors. *Biosens. Bioelectron.* **2012**, *33*, 260–266. [[CrossRef](#)] [[PubMed](#)]
143. Griveau, S.; Dumezy, C.; Seguin, J.; Chabot, G.G.; Scherman, D.; Bedioui, F. In vivo electrochemical detection of nitric oxide in tumor-bearing mice. *Anal. Chem.* **2007**, *79*, 1030–1033. [[CrossRef](#)] [[PubMed](#)]
144. Santos, R.M.; Rodrigues, M.S. Biomimetic sensor based on hemin/carbon nanotubes/chitosan modified microelectrode for nitric oxide measurement in the brain. *Biosens. Bioelectron.* **2013**, *44*, 152–159. [[CrossRef](#)] [[PubMed](#)]
145. Dumitrescu, E.; Wallace, K.N.; Andreescu, S. Real time electrochemical investigation of the release, distribution and modulation of nitric oxide in the intestine of individual zebrafish embryos. *Nitric Oxide Biol. Chem.* **2018**, *74*, 32–38. [[CrossRef](#)] [[PubMed](#)]

